

# A Limit on the Number of Isolated Neutron Stars Detected in the ROSAT Bright Source Catalog

Robert E. Rutledge, Derek W. Fox, Milan Bogosavljevic, Ashish Mahabal<sup>1</sup>

## ABSTRACT

The challenge in searching for non-radio-pulsing isolated neutron stars (INSs) is in excluding association with objects in the very large error boxes ( $\sim 13''$ ,  $1\sigma$  radius) typical of sources from the largest X-ray all-sky survey, the *ROSAT* All-Sky-Survey/Bright Source Catalog (RASS/BSC). We search for candidate INSs using statistical analysis of optical (USNO-A2), infrared (IRAS), and radio (NVSS) sources near the *ROSAT* X-ray localization, and show that this selection would find 20% of the INSs in the RASS/BSC. This selection finds 32 candidates at declinations  $\delta > -39$  deg, among which are two previously known INSs, seventeen sources which we show are not INSs, and thirteen the classification of which are as yet undetermined. These results require a limit of  $< 67$  INSs (90% confidence, full sky, assuming isotropy) in the RASS/BSC. This limit modestly constrains a naive and optimistic model for cooling NSs in the galaxy.

## 1. Introduction

Initial estimates of the number of isolated neutron stars (INSs), accreting through the Bondi (gravitational) mode (Bondi & Hoyle 1944; Bondi 1952), which would be detected in the *ROSAT* All-Sky Survey (RASS) were of the order  $10^3$ – $10^4$  (Treves & Colpi 1991; Blaes & Madau 1993; Madau & Blaes 1994). As observations of higher mean velocities in the radio pulsar population (Lorimer et al. 1997; Hansen & Phinney 1997; Cordes & Chernoff 1998, and references therein) were considered, the predicted number of detectable INSs accreting from the ISM decreased dramatically ( $\sim 10^2$ – $10^3$ ; Colpi et al. 1998; Neuhäuser & Trümper 1999; Treves et al. 2000). This is because the Bondi accretion rate is a strong function of the NS velocity through the interstellar medium (ISM;  $\dot{M} \propto v^{-3}$ ).

---

<sup>1</sup>California Institute of Technology, MS 130-33, Pasadena, CA 91125; rutledge@tapir.caltech.edu, derekfox@astro.caltech.edu, milan@astro.caltech.edu, aam@astro.caltech.edu

Considerable efforts to discover INSs have been applied. Many have used the ROSAT/All-Sky Survey Bright Source Catalog (RASS/BSC; Voges et al. 1999), which contains the 18,811 brightest X-ray sources detected in a survey with the *ROSAT*/PSPC in 1990/1991, with positional certainties of  $\sim 12''$  ( $1\sigma$ ). The survey covers 92% of the sky in the 0.1-2.4 keV band; the RASS sources are complete down to a PSPC countrate of 0.05 c/s, which corresponds to a flux of  $5.4 \times 10^{-13}$  erg cm $^{-2}$  s $^{-1}$  assuming an unabsorbed power-law spectrum of photon index  $\alpha = 1$  (or a flux of  $2 \times 10^{-13}$  assuming  $\alpha = 3$ ). These efforts searched for error boxes which are “empty” of off-band counterparts. INSs have an X-ray to optical ratio of  $\sim 10^5$ , substantially greater than any other class of X-ray sources. The X-ray to optical ratio of a thermal spectrum INS is roughly (Treves et al. 2000):

$$\frac{L_X}{L_{\text{opt}}} \sim 10^{5.5+3 \log\left(\frac{kT_{\text{eff}}}{100\text{eV}}\right)} \quad (1)$$

which is orders of magnitude larger than for other known X-ray source classes; for example, stars typically have  $L_X/L_{\text{bol}} \lesssim 10^{-3}$ , AGN are  $\sim 0.1-10$ , and white dwarfs and X-ray binaries are typically 10–100, but can be as high as 1000. To date, three bright INSs have been optically detected near their expected flux level (Walter & Matthews 1997; Kulkarni & van Kerkwijk 1998; Kaplan et al. 2002). No identified INS has exhibited intensity variability on any timescale.

The predictions for the number of INSs to be detected contrast with only seven such objects reported so far (Treves et al. 2000). This number is so low, that it has been suggested that these INSs are powered not by accretion, but by hot cores of young, cooling NSs (Neuhäuser & Trümper 1999; Popov et al. 2000a). We argue in § 2 that previous analyses have not quantitatively justified their source confusion rates, and the resultant limits on the number of INSs in the RASS/BSC should be held in some doubt.

The INSs which were first cataloged in the RASS/BSC all used ROSAT/HRI localizations ( $\sim 1''$ ) to exclude nearby possible counterparts, and so concentrated on the brightest sources in the RASS. Confusion of optical sources due to the large error-circles of the RASS/BSC hampers INS identification as we discuss in the following section.

In the present work, we obtained a selection of candidate INSs through an expanded application of statistical cross identification (Rutledge et al. 2000), which we summarize in §3 using optical, radio and infrared catalogs. We then present the list of thirty-two candidate INSs, and proceed to exclude sources as INSs when they are shown to be X-ray variable, or have  $L_X/L_{\text{bol}} < 10^4$ . Some are excluded from existing identifications of X-ray variable sources in the literature. *Chandra* X-ray observations which provide arcsec localizations which result in counterpart identifications – or X-ray flux upper-limits,

indicating a variable X-ray source – are described in §4.1; we also describe examination of archival X-ray observations of four sources with ROSAT/HRI, which provide localizations which are also sufficient for identification, or X-ray upper limits for variable sources. In §5, we estimate the upper-limit on the number of INSs detected in the RASS/BSC based on our analysis results, and compare this limit with a naive and optimistic model for a cooling NS source population. A summary and conclusions are given in §6.

## 2. Source Confusion in Previous Work

The observational problem of discovering INSs (for a recent review, see Treves et al. 2000) from the RASS/BSC is severely hampered by source confusion (Motch et al. 1997a; Zickgraf et al. 1997; Bade et al. 1998; Danner 1998a; Danner 1998b; Thomas et al. 1998). For example, the average number of optical sources in the USNO-A2 catalog in a  $3\sigma$  uncertainty region of a RASS/BSC source is  $\sim 3$ , and is often much greater in the Galactic plane. However, at such source densities, an arcsec localization which places the X-ray source coincident with an off-band counterpart results in a probability of random alignment of  $\sim \exp(-\rho\pi(1'')^2) = 0.3\%$ . Thus, an arcsec localization coincident with an optical source in the USNO-A2 argues for association, with a probability of spurious association at the level of 0.3%. For the faintest X-ray sources in the RASS/BSC, the implied  $L_X/L_{\text{opt}}$  for the faintest optical sources in USNO-A2 is  $\sim \text{few}$  – comparable to what is expected for AGN (0.1-10). At higher optical fluxes, the values of  $L_X/L_{\text{opt}}$  approach that of stellar coronae ( $10^{-4}$ – $10^{-3}$ ).

Previous INS searches took the following approach in identifying new INSs: (1) examine off-band source catalogs, images, or spectroscopic surveys for objects which are spatially close to the X-ray source position; (2) all such off-band sources are individually evaluated to be either a plausible counterpart or not; (3) if a plausible counterpart is found, the X-ray source is considered identified as a class which is not an INS.

This approach is a reasonable means for searching for INSs. However, none of the previous works quantitatively assess their confusion rate – specifically: if an INS were placed in one of their fields, what is the probability that they would mis-identify it with a plausible, but incorrect, counterpart?

While the discovered INSs place a lower-limit on the number of INSs in the sky, the upper-limit on INSs in the sky cannot be quantified without knowing the probability of mis-identification. We therefore question the reliability of upper-limits derived from these works. This statistical question is the basis upon which all conclusions regarding the INS

population rests (Neuhäuser & Trümper 1999; Treves et al. 2000; Popov et al. 2000b).

Neuhäuser et al.(1999; N99 hereafter) examined the observed log N-log S curve of INSs, to compare the relative contribution to this curve of INSs powered by Bondi-Hoyle accretion from the inter-stellar medium (ISM) vs. those powered by cooling from their recent ( $<10^6$  yr) SNe. Citing previous work (Bade et al. 1998; Motch et al. 1997a; Motch et al. 1997b), N99 estimated a 2% mis-identification rate; however, we find no quantitative support for this estimation in any of the cited works. The limits derived by N99 for the number of cooling or accreting INSs therefore function only as lower-limits.

We therefore set out in the present work to understand our mis-identification rate, so that we may robustly place an upper limit on the number of INSs in the ROSAT Bright Source Catalog.

### 3. Candidate Source Selection

To produce this selection, we performed a statistical cross-association between the RASS/BSC X-ray sources and sources from three large-area catalogs:

- The National Radio Astronomy Observatory <sup>2</sup> (NRAO) Very Large Array (VLA) Sky Survey (NVSS) catalog (Condon et al. 1998), which contains 1.4 GHz radio sources observed with the Very Large Array radio observatory between 1993 September and 1996 October, with a sensitivity of  $\sim 0.3$  mJy, containing  $\sim 2 \times 10^6$  objects.
- The Infrared Astronomical Satellite (IRAS) Point Source Catalog (v. 2.0) contains  $\sim 250,000$  objects. We use the IR source position, positional uncertainty, and the  $12 \mu\text{m}$  flux density for source flux. The position was taken as the source centroid (precessed from B1950.0 to J2000.0 using the IDL routine `jprecess` from the ASTRO package), and the positional uncertainty was taken as the major axis of the elliptical positional uncertainties.
- The United States Naval Observatory A2.0 (USNO-A2) catalog contains  $\approx 5 \times 10^8$  optical sources, found by scanning optical plates from the Palomar All Sky Survey (POSS-I) at  $\delta > -30^\circ$ , and from the Science Research Council *J* (SRC-J) and European Southern Observatory (ESO-R) survey at declinations below that. We make

---

<sup>2</sup>The National Radio Astronomy Observatory is a facility of the National Science Foundation operated under cooperative agreement by Associated Universities, Inc.

use of the optical source position, positional uncertainty, and quoted  $B$  magnitude. The positional uncertainty of the USNO-A2 catalog is generally  $\sim 0.25''$ , although for objects brighter than 11 magnitude, which saturate the plates, the astrometry is accurate to  $\approx 2''$ . We adopted  $1''$  as the positional uncertainty for each optical source. Based upon an initial investigation, we considered only USNO-A2 sources which were  $< 75''$  from the X-ray source position. The photometric accuracy is estimated as internally 0.15 mag, with systematic errors of 0.25-0.50 magnitudes); however, for our purposes, this is of sufficient accuracy to be useful. We excluded objects with  $B > 20.0$  from consideration.

The approach is described in detail for a cross-association with a single catalog (USNO-A2) elsewhere (Rutledge et al. 2000). Here, we summarize the relevant descriptive elements for the present multi-catalog analysis which produced the initial candidate INS source list.

As we are limited to declinations  $\delta > -39$  deg (the lower-limit of NVSS) we have a total of 15,205 RASS/BSC sources. First, we collect all sources in the three off-band catalogs which are within  $150''$  (except for USNO-A2, where we use  $75''$ ) from the RASS/BSC positions. For each X-ray source  $i$  and off-band source  $j$  pair we calculate a figure of merit  $LR_{i,j;C}$  using a function which is particular to the off-band source catalog  $C$ :

$$LR_{i,j;C} = \frac{\exp^{-r_{(i,j)}^2/2\sigma_{(i,j)}^2}}{\sigma_{(i,j)} N(> F_j; C)} \quad (2)$$

where  $r_{(i,j)}$  is the separation between the X-ray source and the catalog object;  $\sigma_{(i,j)}$  is the uncertainty in  $r_{(i,j)}$ , found by summing the quadrature of the uncertainty in the X-ray position and the off-band catalog object position (taking the largest uncertainty in the case of NVSS, where the uncertainties are typically elliptical); and  $N(> F_j; C)$  is the fraction of sources in catalog  $C$  (actually, in the “background fields”, see below) with greater fluxes than observed from source  $j$ .

In addition to using the single-object catalogs alone, we combined objects in groups of up to three (singles, doubles and triples), so that new “complex” catalogs of multi-source objects were used. For example: we formed complex catalogs of USNO-A2/USNO-A2, USNO-A2/IRAS, USNO-A2/NVSS, NVSS/NVSS and so-on, producing a total of six “doubles” catalogs. For each double-object, the value of  $LR$  is the product of the individual objects which make up the double-object; if one USNO-A2 source had  $LR=5$ , and a second had  $LR=2$ , then the  $LR$  for the “complex” object comprised of both sources had  $LR=20$ ; and similarly for triple-objects.

We then use 24 off-source positions (the “background fields”), offset in a  $5 \times 5$  grid with separations of  $300''$  and radii of  $150''$  (except USNO-A2, where we use  $75''$ ). We exclude background fields which contain RASS/BSC sources. We calculate  $LR_{i,j;C}$  for those “pairs” using now the center of the blank fields as the X-ray “source” position. Then, we calculate a “reliability”  $R$  for each pair  $i, j; C$ :

$$R_{i,j}(LR_{i,j;C}) = \frac{N_{\text{src}}(LR_{i,j;C}) - N_{\text{background}}(LR_{i,j;C})}{N_{\text{src}}(LR_{i,j;C})} \quad (3)$$

where  $N_{\text{src}}(LR_{i,j;C})$  is the number of objects in the source fields which had a value  $LR$  within a  $\delta LR$  of that obtained for the pair  $i, j$ , and  $N_{\text{background}}(LR_{i,j;C})$  is the same, but in background fields. The value  $R$  is a pure probability – the probability that the candidate counterpart  $j$  is not a background object, but is associated with the X-ray source in some way (and not necessarily as the X-ray emitter).  $R$  is independent of the source catalog  $C$  or the nature of the object  $j$ , and so we now can mix the values of  $R$  for the same X-ray source  $i$  to produce the probability that off-band source  $j$  is associated with the X-ray source exclusive of other off-band sources in the field:

$$P_{i,\text{id}} = \frac{R_{i,j} \prod_{j' \neq j} (1 - R_{i,j'})}{K} \quad (4)$$

Similarly, the probability that none of the objects in the field are associated with the X-ray source  $i$  is:

$$P_{i,\text{no-id}} = \frac{\prod_j (1 - R_{i,j})}{K} \quad (5)$$

and the normalization  $K$  is:

$$K = \prod_j (1 - R_{i,j}) + \sum_j R_{i,j} \prod_{j' \neq j} (1 - R_{i,j'}) \quad (6)$$

When  $P_{i,\text{no-id}}$  is close to 1, none of the off-band objects in the field have properties which demonstrate a statistical excess in X-ray fields over background fields – that is, the off-band objects in the field are beyond the confusion limit. As found previously (Rutledge et al. 2000), typical uncertainties in the values of  $P_{\text{id}}$  and  $P_{\text{no-id}}$  are  $\sim 2\%$ .

In performing this analysis, we also inserted 150 “control” sources among the source fields, set randomly about the sky in proportion to the local X-ray source density within our survey area. These act as a control experiment – since they are not real sources, they

will have no detectable off-band counterparts in the all-sky catalogs, just as for INSs. This permits us to evaluate the efficiency with which our statistical selection will identify real INSs. Of the 150 “control” sources, 29 were found with  $P_{\text{no-id}} > 0.90$  by this procedure; the remaining 80% of the control sources had  $P_{\text{no-id}} < 0.90$ , due to confusion with nearby optical sources.

In Fig. 1a, we show the spatial distribution of the control fields in Galactic coordinates. In Fig. 1b, we show the 29 fields found with  $P_{\text{no-id}} > 0.90$ . While the control fields are evenly distributed about the sky in our survey region, the “found” fields clearly avoid the Galactic plane. This is due to the fact that so many optical point sources populate the plane, that the fields are confused with spurious (low significance) sources (Fig. 1c).

In Fig. 1d, we show the cumulative distribution  $N(< |b|)$  of the control sources with  $P_{\text{no-id}} > 0.90$ , in comparison with one expected from an equal area distribution in  $|b|$  (taking into account the declination constraint for our survey area, which makes a difference only at the  $\sim$ few percent level in the cumulative distribution). Note that no control fields are found with  $|b| < 20$  deg. Using a K-S test (Press et al. 1995), the detected control sources are inconsistent with an equal area distribution (KS probability of  $\text{prob}_{\text{KS}} = 3 \times 10^{-6}$ ), which we attribute to source confusion in the Galactic plane. Modeling the absent sources as a correction of  $F(b) = \sin^n(b)$ , we find 90% confidence limits on  $n$  of 1.25-3.8, with a best value of  $n = 2.2$ .

### 3.1. Source Selection

We began with objects for which  $P_{\text{no-id}} > 0.90$  (60 objects). From these, we excluded all objects in which the RASS/BSC hardness ratio HR1 indicated an effective temperature  $> 200$  eV (28 sources), which are too spectrally hard to be cooling or Bondi-accreting INSs. In the RASS/BSC, HR1 is defined in the usual fashion ( $= (B-A)/(B+A)$ ), where B is the number of counts detected in the 0.5-2.0 keV band, and A is the number of counts detected in the 0.1-0.4 keV band), and we require  $\text{HR} > 0$ . Because Bondi-accreting or cooling INSs are expected to have lower effective temperatures than 200 eV, we expect to lose no INSs from this cut (previously known INSs also have effective temperatures  $< 200$  eV). The thirty-two candidate sources are listed in Table 2, along with their number in the ROSAT Bright Source (RBS) catalog (Fischer et al. 1998; Schwobe et al. 2000a; Fischer et al. 2002), and other particulars as we describe in this section.

We show in Table 1 the calculated values of  $P_{\text{id}}$  for the seven known INSs listed in Treves et al. (2000), plus one more identified more recently (Zampieri et al. 2001). Three are

at declination below the NVSS limit, and so were not included in our analysis. Three have optical sources in the field which have probabilities of being the counterparts which would have selected them out of our sample. Two more, as we stated above, have a  $P_{\text{no-id}} \sim 1$ , such that they would have been included in our sample for *Chandra* observations. This lends confidence that our approach is capable of selecting INSs, although – as expected – source confusion hampers discovery.

### 3.2. Source Classification

We classify the thirty-two sources into one of three classes: (1) an INS; (2) not an INS; (3) undetermined. These classifications are listed in column 6 of Table 2, with the relevant reference for their classification in column 7. Here, we discuss the classifications each in turn.

Two of these sources are previously identified INSs.

A source is definitively not an INS when either: (a) it is localized to  $\sim 1''$  (with either a *Chandra* or ROSAT/HRI localization), and there is a spatially coincident optical counterpart with  $L_X/L_{\text{bol}} < 10^4$ ; or (b) the X-ray source is variable on any timescale.

Finally we regard the classification as undetermined when the X-ray localization is not at the  $1''$  precision level, and when the X-ray source has not been shown to vary in intensity.

We first examined the SIMBAD-listed identifications and classifications for these sources (see Table 2). From these sources, we examined the literature for observations in which the X-ray source was shown to vary in intensity. We found five such sources in our list, which we classify as not INSs.

We obtained 1 ksec *Chandra*/HRC-S observations of eight selected fields. As we describe in § 4.1, in all cases we found either off-band counterparts at the arcsec *Chandra* positions, or that the X-ray sources were variable, resulting in a classification of “not an INSs”.

Four of the remaining sources had ROSAT/HRI observations in the archive. Using these, we show that either the sources were variable, or could be identified with an off-band counterpart using the  $\sim$ few arcsec localization (see § 4.2) and are therefore not INSs.

We found thirteen sources with either previous identifications but no evidence of X-ray variability; or for which there were nearby ( $\lesssim 30''$ ) off-band sources which belong to classes which are known X-ray emitters, which we list as possible counterparts. We classify these



sources as “undetermined”.

Following these classifications, we find: 2 INSSs, 17 sources which are not INSSs, and 13 with undetermined classification.

## 4. X-ray Observations and Analyses

In this section, we describe the X-ray observations on which we rely to provide the arcsec localizations, demonstration of X-ray variability, and subsequent classifications as “not an INS”. The *Chandra* observations are part of an observing program to search for INSSs, and so we describe these observations in some detail in § 4.1. The *ROSAT* observations, taken from the public archive, are more summarily described in § 4.2.

### 4.1. *Chandra* Observations and Analysis

All observations were performed with the HRC-S in imaging mode. Details of each observation are in Table 1. All analyses were performed with CIAO v2.2<sup>3</sup>. *Chandra* source localizations were performed with `wavdetect`, by binning the data by a factor of 8 (1.05'' per bin), and searching for sources on scales of 1, 2, 4, 8, and 16 bins (1.05-16.9''), with significance threshold of  $10^{-6}$ . Upper-limits to the average countrate, when no source is detected, are found by rebinning the area within 2' of the *ROSAT* position to 2.1'' wide bins, and finding the greatest number of counts/bin. All detected X-ray sources were found on the smallest wavelet scale (1.05'') indicating that none were extended.

Here, we detail the results of individual X-ray source searches, and individual optical counterpart identifications. Where we find an X-ray source in our *Chandra* data, we search for optical counterparts in the Digitized Sky Survey (DSS), IR counterparts in the 2MASS 1st and 2nd incremental databases (which cover  $\sim 40\%$  of the sky, for which astrometry and photometry are available) the 2MASS quicklook image database (which cover 100% of the sky, but without astrometry and photometry), and in the Digitized Palomar Sky Survey (DPOSS; Djorgovski et al. 1998).

As the RASS/BSC error circles are typically  $> 8'' (1\sigma)$  and there is typically 1 optical source in these fields localized to 1'', the *a priori* probability that any X-ray source will spatially coincide with an unassociated optical source is  $< 0.5\%$ . We therefore do not expect

---

<sup>3</sup><http://asc.harvard.edu/ciao/>

any spurious spatial associations with optical sources.

We estimate fluxes assuming a steep photon spectral slope of  $\alpha = 3$  and X-ray column  $N_{\text{H}}=0$ , for which 1 *Chandra*/HRC-S count =  $1.4 \times 10^{-12}$  erg cm<sup>2</sup> (0.5-2.0 keV).

The analysis results for the individual targets are as follows.

**1RXS J020317.5–243832.** Two X-ray sources are found in this field, both of which lie close to optical point sources in the DSS. As this offers the opportunity to do much better astrometry, we handled the absolute astrometry of this source slightly differently from our other targets. We correct the X-ray aspect according to the *Chandra* X-ray Science Center prescription <sup>4</sup>, which has typical  $1\sigma$  systematic uncertainty of  $0.6''$ . We rebinned the X-ray data by only a factor of 2, and used `wavedetect` to obtain localizations, which were relatively accurate with a precision of  $0.04''$  for the and  $0.09''$  for 1RXS J0203–2438 and the second object, respectively. Both can be identified with optical sources in the DSS, as well as in a 5-min integration image taken with ESI at Keck II shown in Fig. 2. To perform absolute astrometry, a 30-sec exposure of the field was also obtained with ESI/Keck II; six Guide Star Catalog II stars over this field were used to provide an absolute astrometric registration of  $0.25''(1\sigma)$ ; the 5-min exposure was then registered relative to the 30-sec exposure. Finally, the second X-ray source in the field was assumed to be exactly coincident with an optical point source in the field – which coincided with the X-ray position to within *Chandra* astrometric errors ( $0.6''$ ). The *Chandra* source corresponding to the RASS/BSC object is CXO 020317.626-243837.8, with an absolute uncertainty in its position of  $\pm 0.3''$ . The corresponding optical source is near the plate limit on the DSS blue plate, and is not listed in the USNO-A2 catalog, nor is it detected in the 2MASS quicklook images. Taking the DSS plate limit to be  $B=20.8$  (the faintest of 10 objects within  $100''$  of the X-ray source, listed in USNO-A2), and assuming the optical source to have a magnitude equal to this limit, this sets an  $L_X/L_B \approx 2$ , with fractional uncertainties at the level of 50%, due to uncertainty in the optical flux near the plate limit. This is consistent with an AGN origin for this object, which we offer as a tentative classification.

We observed the optical counterpart with the 10 m Keck II telescope and Echelle Spectrograph and Imager (ESI) on 5 November 2002 UT. In its echelle mode ESI provides uniform  $11.5 \text{ km s}^{-1} \text{ pixel}^{-1}$  spectral resolution in the 4000–11,000 angstrom wavelength range. A single 600 s spectrum of the source reveals a broadband continuum with no prominent emission lines, and thus does not help much to clarify either the nature of the source or its distance or redshift.

---

<sup>4</sup>[http://asc.harvard.edu/calASPECT/fix\\_offset/fix\\_offset.cgi](http://asc.harvard.edu/calASPECT/fix_offset/fix_offset.cgi)

**1RXSJ 024528.9+262039.** The *Chandra* X-ray source is spatially distant ( $22.7''$ ,  $2.8\sigma$ ) from the RASS/BSC position, and is coincident with a bright IR source, detected in 2MASS and listed in USNO-A2. Our statistical analysis had placed a probability of unique identification with the USNO-A2 object of  $P_{\text{id}}=0.088$ , due large distance from the ROSAT X-ray position. The corresponding USNO object has  $B = 14.8$ , so  $J - K=0.93$  and  $B - K=6.2$ . The colors are appropriate to a late M-type star (M3 has  $B - K=6.1$ ,  $J - K=1.07$ ; M4 has  $B - K=6.43$ ,  $J - K=0.90$ , well within errors; Zombeck 1982). For the  $V - J$  and bolometric correction of an M3 star (B.C. =  $-2.03$ ;  $V - J=3.66$ ), we find  $L_X/L_{\text{bol}}=6\times 10^{-3}$ .

We tentatively classify this X-ray source as a coronally active star of spectral type M2-M4. The absolute J magnitude is then  $M_J = 6.98 - 8.34$  (Hawley et al. 2002). The implied distance modulus is  $m_J - M_J=1.11-2.47$ , or a distance between 16 and 31 pc. The implied X-ray luminosity is  $(2-6)\times 10^{27}$  erg s $^{-1}$ .

**1RXS J115309.7+545636.** There is no X-ray source detected in the *Chandra* field. We find an X-ray average countrate upper-limit of  $<4.7$  c/ksec, and  $F_x <7\times 10^{-15}$  erg cm $^{-2}$  s $^{-1}$ . At the time of analysis, there was an undocumented hot pixel in the detector, which was  $>2'$  from the RASS/BSC source position, and which does not affect our analysis.

The X-ray source was present in pointed observations with ROSAT/PSPC on 1996 June 25, listed in the WGA catalog (White et al. 1994) with a countrate of 27 c/ksec, approximately a factor 5 fainter than during the RASS ( $130\pm 20$  c/ksec). Thus, the object is variable on at least a 5-year timescale. At the fainter flux of the pointed ROSAT observation, this object would have been only marginally detected (with  $\sim 6$  counts) with the HRC-S.

**1RXS J122940.6+181645.** There is no X-ray source detected in the *Chandra* field. Based on the source hardness ratio and PSPC countrate, this was predicted to be the brightest object in the survey, with 400 counts/ksec. We find no  $2''$  regions within a  $2'$  radius of the RASS position with more than 3 counts, corresponding to an observed average X-ray countrate upper-limit of  $\leq 2.7$  c/ksec, and  $F_X \leq 4\times 10^{-15}$  erg cm $^{-2}$  s $^{-1}$ . The observed X-ray limit indicates this source has faded by 2 orders of magnitude from the average X-ray flux observed during the RASS.

The ROSAT source has been tentatively identified as a BL Lac-type object RBS 1116 of unknown redshift (Schwope et al. 2000b), with  $V=20.5$  found from folding a low resolution spectrum with the sensitivity curve of a  $V$  filter, in the process of the Hamburg survey for quasars in the RASS/BSC (Bade et al. 1998). In a  $3''$  circle centered at the location of this optical source given in Schwope et al. (2000b), we find 1 count (with 1.0 background

counts expected); this implies an upper-limit to the average countrate of the source of  $< 5$  counts/ksec or  $F_X < 7 \times 10^{-15}$  (96.6% confidence), and  $F_X/F_V < 0.3$ .

**1RXS J132833.1-365425.** This was the brightest detected X-ray source in this survey, with  $687 \pm 25$  c/ksec, a factor of 10 brighter than predicted from the RASS/BSC countrate. Visual examination of the X-ray lightcurve showed no evidence for variability on a 1 or 100 second timescale. The X-ray source position (Fig. 3) is coincident with an IR source in the quicklook 2MASS images (Epoch 1999.45; 2MASS catalog photometry and astrometry is not yet available); we associate the *Chandra* X-ray source with this IR source. The nearest DSS object is  $\sim 4.3'' \pm 1''$  away, in an image taken in epoch 1975.27; although the source is well above the DSS plate limit, it is not listed in USNO-A2, for reasons which are unclear. The source is listed in the GSC 2.2, with  $B=15.42 \pm 0.17$ . A plate taken during the Second Epoch UK Schmidt survey shows that the earlier epoch source has measurable proper motion, consistent with that object being at the location of the 2MASS source at the Epoch of the 2MASS observation. The implied proper motion is 165 milliarcsec/yr, with a  $1\sigma$  25% uncertainty due to *Chandra* absolute astrometric uncertainties, indicating the source is a nearby, low-mass star.

**1RXS J145010.6+655944.** There is a faint source visible in the DSS2 blue plate, within  $1''$  of the *Chandra* X-ray source position. However, it is not detected on the red plate, and it is not included in USNO-A2. It is also detected by DPOSS (Fig. 4). There is no 2MASS source at the X-ray position in the 2MASS quicklook images. An optical spectrum of this source was taken with Keck in May 2002 (Fig. 5). The spectrum shows several narrow emission lines. We identify the object as a cataclysmic variable (CV) on the basis of its  $H\alpha$  line (compare, for example, with spectrum from SDSS 1555, Szkody et al. 2002).

**1RXS J145234.9+323536.** No X-ray point source was detected in the *Chandra* observation. This position on the sky has not otherwise been observed with the ROSAT, ASCA, or SAX X-ray observatories. Binning the  $2'$  circle around the source position into  $2.1''$  pixels, the largest number of counts per pixel was 3, for an upper-limit to the average countrate of  $< 2.3$  c/ksec, or  $F_X < 3 \times 10^{-15}$  erg cm $^{-2}$  s $^{-1}$ . This is a factor of 44 below the predicted countrate.

**1RXS J163910.7+565637.** The X-ray source is associated spatially with an optical source (Fig. 6) near the center of the error box in DPOSS. The source is also observed near the survey limit in 2MASS quicklook images. The source is detected in the DSS blue and red plates, but it is not listed in USNO-A2, possibly due to extendedness. It is, however, listed in the HST Guide Star Catalog 2.2 as source N11231206454, with  $B=17.8 \pm 0.42$ ; this corresponds to a flux ratio  $F_X/F_B \sim 0.1$ , comparable to those expected for AGN.

An optical spectrum taken with Keck/LRIS in May 2002 showed a broad emission line ( $\sim 4000 \text{ km s}^{-1}$ )  $\lambda$  at  $7412\text{\AA}$ . If this is identified with MgII, then the redshift of the source is  $z = 1.65 \pm 0.01$ . Assuming a Hubble constant  $H_0 = 65 \text{ km s}^{-1}$ ,  $\Omega_\Lambda = 0.7$  flat universe, the intrinsic X-ray luminosity is  $1.4 \times 10^{45} \text{ erg s}^{-1}$  (in the observed 0.5-2.0 keV band). Assuming a K-correction of 2 mag, the absolute  $B$  magnitude is  $M_B = -29.8$ .

#### 4.1.1. Comparison of Chandra results, RASS/BSC Positions, and USNO-A2 Sources in the Digital Sky Survey

In Fig. 7, we show the eight fields of our INS candidates, taken from the Digital Sky Survey (DSS). The RASS/BSC error circle ( $3\sigma$ ) is shown for each source, as well as the *Chandra* localization for the five sources which were detected. Of the three X-ray sources associated with AGN, two (1RXS J0203-2438, 1RXS J1450+6559) have optical counterparts which were at or below the DSS plate limit; the third (1RXS J1639+5656) has an optical counterpart which is well above the plate limit but which was not listed in USNO-A2, possibly due to its extendedness. Finally, of the two sources which are associated with stars, one (1RXS J0245+2620) was listed in USNO-A2, but was close to  $3\sigma$  from the RASS/BSC position, and so had a low probability of association ( $P_{\text{id}}=0.088$ ). The other (1RXS J1328-3654), which was  $< 1\sigma$  from the RASS/BSC position, is not listed in USNO-A2.

Had the optical counterpart of 1RXS J1639+5656 been included in USNO-A2, we find that it would have had  $P_{\text{id}} \sim 0.70$ , and would not have been included in our selection. Similarly, the optical counterpart to 1RXS J1328-3654, had it been included in USNO-A2, would have had  $P_{\text{id}}=0.85$ . As such, neither would have ended up in our selection as INS candidates. The other optical counterparts which did not appear in USNO-A2 were well below the optical confusion limit, and would have had  $P_{\text{id}}=0$ .

## 4.2. ROSAT HRI Observations and Analysis

Four sources in our list have archived ROSAT/HRI observations. We examined each in turn, using data from the HEASARC ROSAT archive at GSFC. We took positions and countrates from the first ROSAT Source Catalog of Pointed Observations with the High Resolution Imager<sup>5</sup>, while estimating upper-limits to countrates from the raw

---

<sup>5</sup>ROSAT Consortium, ROSAT News No. 74, 2001 Aug 9

data. Although the X-ray focusing capability of the ROSAT/HRI permits relative X-ray localization to  $1''$ , there is a systematic uncertainty in the absolute positions derived from ROSAT/HRI observations at the level of  $\sim 3''$  due to a boresight uncertainty, which must be kept in mind during analysis.

**1RXS J094432.8+573544.** A 3.4 ksec HRI observation (RH704086N00) detects both this and a second X-ray source, with  $\sim$ arcsec precision (at 09h44m31.s8+57d35m38s and 09h44m01.s9+57d3m210s respectively). Comparing these sources with DPOSS images finds that they can be re-registered with an offset consistent with the known ROSAT/HRI boresight uncertainty. Source 2 corresponds to USNOA2 094402.52+573209.2 ( $B = 17.4$ ,  $V = 17.7$ ); re-registering the X-ray source to 09h44m32.s42+57d35m37.s2 finds that it corresponds with DPOSS 094432.42+573534.9 with  $(g,r,i)=19.68,20.59,20.11$ ), with an offset of  $2.9''$ . There are four sources in the DPOSS catalog with  $g > 20.0m$ , within a  $120'' \times 120''$  box of this source. The probability of chance alignment at  $2.9''$  of one of these sources is 0.7%. The optical counterpart is too bright to correspond to an INS, and so we identify the X-ray source as not an INS. Its  $L_X/L_{opt}$  ratio is comparable to that of known AGN, and therefore this source may be an AGN.

**1RXS J130547.2+641252** During the one 1.6 ksec HRI observation (RH704083N00), the source was undetected ( $<3$  counts) within a  $60''$  radius of the RASS/BSC position. The RASS/BSC countrate ( $0.17 \pm 0.02$  PSPC c/s) corresponds to 0.054 HRI c/s (assuming a power-law photon spectrum  $\alpha = 3$ ), or 87 counts during this observation, indicating that the source has faded by a factor of  $\gtrsim 30$ . Based on this variability, we identify the source as not an INS.

**1RXS J130753.6+535137** This X-ray source has been identified (from spatial coincidence) with the very well studied CV V\* EV UMa. A 11.9ksec HRI observation (RH300382N00) does not detect the X-ray source within  $60''$  of the RASS/BSC position ( $< 5$  counts). Based on the RASS/BSC countrate ( $1.86 \pm 0.06$  PSPC c/s), the predicted number of counts in the HRI observation is 7100, indicating that the source has faded by a factor  $\gtrsim 1400$ . Based on this variability, we identify the source as not an INS.

**1RXS J163421.2+570933** We examined HRI observations centered on this source (RH201944N00 and RH202224N00, epochs 1995.27 and 1996.24 respectively) for which the source is focused within the central  $1'$  of the observation. The X-ray source is detected in both observations. In the latter observation, its arcsec localization was 16h34m21.17s+57d09m38s. We examined the 2MASS J-band quick-look image (epoch 1999.36) and DSS V-band images from two epochs (epochs 1955.32, 1991.50). We find a high proper-motion binary, with two components separated by  $37''$ . The southern component (2MASS J163420.44+570944.0, – a (J,H,K)=8.50, 8.04, 7.77m, with colors

corresponding to a K5-7 dwarf, or a K2 giant) – moves with  $(\mu_\alpha, \mu_\delta) = (-1135 \pm 5, +1170 \pm 30)$  mas/yr, which places it at 16h34m20.87s+57d09m40.3s at the epoch of the ROSAT/HRI observation, which is  $3.4''$  away from the ROSAT/HRI position, within the boresight correction uncertainties. The northern component is 2MASS 163421.6+57108.2, with  $(J, H, K) = (14.09, 14.08, 14.07)$  – a flat spectrum, possibly corresponding to an A-type star. There are 15  $K < 7.77$  point sources in 2MASS, within 1 degree of this position, and the probability of one falling at  $< 3.4''$  from the ROSAT position randomly is  $1.3 \times 10^{-5}$ . Based on the low likelihood of positional coincidence, we associate the X-ray source with 2MASS J163420.44+570944.0 and identify it as not an INS.

## 5. Estimation of the Number of INSs Detected in the RASS/BSC

To place a limit on the total number of INSs detected among the 18,811 X-ray sources in the RASS/BSC, we model the selection of our candidate list, and correct for each step.

**Step 1: Statistical selection of INSs:** As described in § 3, we performed a statistical cross identification with the intention of finding INSs from the absence of any likely off-band counterparts, as quantified by  $P_{\text{no-id}} > 0.90$ . From the original 15,205 RASS/BSC sources above our declination cut, 60 X-ray sources passed this selection. Of  $A = 150$  “control” sources,  $B = 29$  passed our  $P_{\text{no-id}}$  selection. A real INS in our survey region has a probability  $p$  of passing our INS selection; we represent this value  $p$  as a binomial distribution (Fig. 8):

$$P_{\text{XID}}(p) = \frac{p^B(1-p)^{A-B}}{\int_0^1 p^B(1-p)^{A-B} dp} \quad (7)$$

**Step 2, Spectral Hardness Cut:** We selected a total  $T = 32$  (from 60) X-ray sources with spectral hardnesses corresponding to effective temperatures  $kT_{\text{eff}} < 200$  eV, which we assume loses no INSs since cooling and accreting (non-magnetic) INSs have effective temperatures below this value (Popov et al. 2000a).

**Step 3: Candidate Classification:** After examining the literature, X-ray variability history, and new arc-sec localizations, we classified all  $T = 32$  candidates as either an “INS” (2 sources), “not an INS” (17) or “undetermined” ( $BG = 13$ ). We discovered no new INSs among our candidates. However, any (or all) of the  $BG$  objects may well be INSs. We require a correction, which is the (un-normalized) probability  $P_{BG}(N)$  that a number  $N$  sources in the  $T = 32$  selection are INSs, with only  $N_{\text{INS,min}} = 2$  INSs so identified:

$$P_{BG}(N) = \frac{\binom{N}{N_{\text{INS},\text{min}}} \binom{T-N}{T-BG-N_{\text{INS},\text{min}}}}{\binom{T}{T-BG}} \quad (8)$$

Here  $N_{\text{INS},\text{min}} \leq N \leq N_{\text{INS},\text{max}}$  – that is,  $N$  ranges from the minimum number of INs known to be present in our sample of  $T$  objects to the maximum number of INs which could be present in the sample of  $T$  objects ( $N_{\text{INS},\text{max}} = N_{\text{INS},\text{min}} + BG = 19$ ). See Fig. 9. The function  $\binom{x}{y}$  is the familiar combinatorial factor  $x!/(y!(x-y)!)$ .

These selections combined produce the unnormalized probability  $P_{\text{INS}}(M')$  that the total number of INs in our survey field is  $M'$ :

$$P_{\text{INS},\text{un-normalized}}(M') = \sum_{N=N_{\text{INS},\text{min}}}^{\min(M', N_{\text{INS},\text{max}})} \left( \frac{P_{BG}(N)}{\sum_{N=N_{\text{INS},\text{min}}}^{\min(M', N_{\text{INS},\text{max}})} P_{BG}(N)} \int_0^1 P_{\text{XID}}(p) \frac{p^N (1-p)^{M'-N}}{\int_0^1 p^N (1-p)^{M'-N} dp} dp \right) \quad (9)$$

where  $\min(A, B)$  takes the lesser value of  $A$  and  $B$ . To produce the probability that there are  $\geq M$  INs in our survey field, we sum:

$$P_{\text{INS}}(\geq M) = \sum_{M'=M}^{\infty} \frac{P_{\text{INS},\text{un-normalized}}(M')}{\left( \sum_{M'=N_{\text{INS},\text{min}}}^{\infty} P_{\text{INS},\text{un-normalized}}(M') \right)} \quad (10)$$

We begin the summation for the number of INs in our fields at  $M = 2$  since this is the number of INs we would have found with arc sec *Chandra* localizations. This results in upper-limits on the number of INs detected in the RASS/BSC in our survey area of 56 (90% confidence – that is,  $P_{\text{INS}}(\geq 56) = 0.1$ ) and 87 (99% confidence). These limits are consistent with the number of INs previously known to be in our survey area (five).

A perhaps more intuitive (but less precise) way to obtain this limit is the following. We ultimately found 2 INs. The combinatorial probability (Eq. 8, Fig. 9) shows that there can be at most 9 INs (90% confidence) in the selection of 32. Our control fields showed (Eq. 7, Fig. 8) that for every 1 IN we find in our selection there are five INs in our survey area. Thus, the 90% upper-limit of 9 in our selection becomes an upper-limit of  $5 \times 9 = 45$  in our survey area. After adding an additional 20% due to the width of our “control” field selection distribution (Fig. fig:pxid), the 90% upper-limit is 55 INs in our survey area, comparable to the upper-limit of 56 we found in the more precise calculation.



Thirteen of the RASS/BSC sources in our sample did not have either an  $\sim$ arcsec position, or demonstrate X-ray variability, to rise to the level of being definitively classified as “not an INS”. All thirteen had previously been examined by other workers, who had found some nearby off-band source in the error-circle with which the X-ray source may plausibly be identified. While we do not accept these associations due to the absence of quantitative association argument, if one accepts these suggested associations, then the upper-limits on the number of INSs in our survey field decrease to  $<34$  and  $<56$  (90% and 99% confidence, respectively).

### 5.1. Full-Sky Number of INSs in the RASS/BSC, Assuming Isotropy

Since the effects of the galactic-latitude dependent confusion are already accounted for in our estimation of  $p$ , we do not need to account for this in calculating the correction for the full-sky, isotropic number of INSs in the RASS/BSC. Correcting only for the ratio of area coverage (a factor of 1.2) we find there are  $<67$  and  $<104$  INSs at 90% and 99% confidence. These limits are consistent with the number of INSs in the full sky RASS/BSC (seven).

### 5.2. Comparison of Observed Limit on INSs with a Naive and Optimistic Cooling NS Model

Here, we compare this limit on the number of INSs in the RASS/BSC with a naive and optimistic model for cooling INSs in the galaxy.

We assume that such INSs are produced in the disk at a rate of  $\gamma_{-2}$  per 100 years, out to a radius of  $R_{\text{disk}}=15$  kpc; that such INSs have a velocity perpendicular to the disk, which remains constant in time, of a magnitude  $V_{\text{perp.}}$ ; that the disk can be treated in this limit as an infinite plane; that the X-ray luminosity is  $2 \times 10^{32}$  erg s $^{-1}$  in the ROSAT/PSPC passband (0.1-2.4 keV) for  $\tau = 10^6$  yr, after which the luminosity is zero (see, for example, Yakovlev et al. 2001); and that the flux limit is  $2 \times 10^{-13}$  erg cm $^{-2}$  s $^{-1}$ , which permits the detection of such INSs to a distance of  $\chi_{\text{lim}}=10.3$  kpc. In this model, the number of detected NSs is:

$$N = \frac{\gamma_{-2}(0.01 \text{ yr}^{-1})}{\pi R_{\text{disk}}^2 V_{\text{perp.}}} 2\pi \int_0^{\min(V_{\text{perp.}}, \tau, \chi_{\text{lim}})} \int_0^{\sqrt{\chi_{\text{lim}}^2 - z^2}} R dR dz \quad (11)$$

where  $R$  is the distance of the INS from the observer in the Galactic plane and  $z$  is the

distance of the INS above the Galactic plane. This model is optimistic, in that it assumes that the INSs all have temperatures which are at the very upper-limit of theoretical estimates.

There are several reasons why this model is naive. First, it neglects the effect of absorption in the plane of the galaxy, which cannot be neglected for spectrally soft X-ray sources which would be observable out to 10 kpc. Second, it parameterizes the velocity perpendicular to the disk as a delta-function, while it is known that the radio pulsars are observed to exhibit a range of velocities, and the NSs will naturally travel with a distribution of angles relative to the disk.

Nonetheless, a limit of  $<67$  INSs in the RASS/BSC in this model produces a limit on  $\gamma_{-2} < 0.025$  (90% confidence), for  $V_{\text{Perp.}} < 10 \text{ kpc Myr}^{-1}$ , or a hot NS birthrate of 1 per 4000 years. This is low compared with the estimated SNe rate ( $\gamma_{-2} \sim 1$ ), and most likely implies that the naive and optimistic assumptions for this model are incorrect. Popov et al. (2000a), for example, have examined a cooling NS population model which includes galactic absorption, showing its effect to be important.

If we assume an  $\alpha = 3$  spectrum with a column density  $N_{\text{H}} = 3 \times 10^{21} \text{ cm}^{-2}$  (slightly above the median all-sky value; Dickey & Lockman 1990), the unabsorbed flux limit is substantially greater:  $9 \times 10^{-12} \text{ erg cm}^{-2} \text{ s}^{-1}$ , for which INSs could be detected out to a distance of 1.5 kpc. Assuming an average spatial H density of  $1 \text{ cm}^{-3}$ , the column density out to such distances is  $4.5 \times 10^{21}$  – comparable to our assumed  $N_{\text{H}}$ . Under this assumption, our limit on  $\gamma_{-2} < 1.1$ .

Comparison of the present results with this naive and optimistic model demonstrates that the limit on the number of INSs obtained is sufficient for detailed comparison with the INS model population under a range of assumptions (birth-rate, velocity distribution, NS cooling models, galactic distribution). We leave detailed comparison of these observational results with realistic population models for future work.

## 6. Summary and Conclusions

We performed a selection of INS candidates, and examined them for identification as INSs. We showed that this selection should identify 20% of the INSs in the Galaxy; confusion of USNO-A2 sources in the plane of the Galaxy is the major barrier efficient INSs identification. The selection found 32 candidate sources; of these, two were previously known to be INSs, seventeen we determine to be not INSs, and thirteen we leave as undetermined classification. No new INSs were discovered.

This results in limits for the number of INSs detected in the ROSAT/BSC of <67 INSs full sky (90% confidence) or <104 INSs full sky (99% confidence).

Of eight RASS/BSC X-ray sources observed with *Chandra*, three have faded, by factors of 5, 44, and 100; two are associated with tentatively classified low-mass stars, one is a CV and the remaining two are tentatively classified as AGN. Of the four observed with the ROSAT/HRI, we find that one faded by a factor of  $\gtrsim 30$ ; one – previously identified as a CV – also faded by a factor of  $\gtrsim 1400$ ; the remaining two are a high-proper-motion binary, and a source which may be an AGN.

The classification of four fading sources is uncertain. One (1RXS J1229+1816) has previously been suggested to correspond to a BL Lac object in the field; we have no additional evidence of that, except that BL Lac objects are known to vary dramatically in the X-ray, and this X-ray source faded by a factor  $> 100$ .

If most INSs are powered by NS cooling as in the first  $10^6$  yr following supernova, then the assumption of an isotropic distribution is well justified. On the other hand, if most INSs are powered by accretion from the ISM, one might expect a greater concentration of INSs toward the plane, as the ISM has a scale-height of  $\sim 300$  pc; however, because the mass accretion rate in Bondi accretion is strongly velocity dependent  $\dot{M} \propto v^{-3}$ , and the mass accretion rate in magnetically dominated accretion is dependent on the velocity with the *opposite* sense as Bondi accretion ( $\dot{M} \propto v^{1/3}$ ), as well as on the NS magnetic field strength (Rutledge 2001; Toropina et al. 2001), correcting for a non-isotropic population is model-dependent, and we leave this for future work.

Note that our statistical cross-association technique excludes sources from consideration when the X-ray sources are associated with off-band counterparts. This is a reasonable approach if the INSs are not in any way associated with – for example – optical sources. If, however, most INSs were born with low velocities, then they may stay near their birthplace which may therefore be associated with bright optical sources such as an OB association. If this were the case, then we would miss such INSs, and our limit does not apply to these. If, however, NS formation or evolution processes give rise to a peculiar velocity of  $\sim 100$   $\text{kms}^{-1}$ , the INS will have crossed a galactic disk width (100 pc) on a timescale comparable to the cooling time ( $10^6$  yr), so that it would not be associated with its birthplace.

The present limits on the number of INSs in the RASS/BSC are quantitatively comparable to those obtained from previous surveys (Neuhäuser & Trümper 1999, and references therein). However, the limits from previous surveys were found by estimating a confusion rate with a spurious background AGN or stars; these estimates (typically  $\sim$  few percent) were not based on any quantified analysis of the non-X-ray AGN or stellar presence

in background fields. In the present analysis, we quantified the confusion rate for INSs in our survey field by using control sources, finding that  $\sim 80\%$  of INSs would be confused with background sources. We therefore believe our estimation of the confusion rate to be highly robust in comparison to previous results, and our limits on the INSs in the RASS/BSC to be robust as well.

The fact that all X-ray sources detected with *Chandra* or *ROSAT*/HRI yielded an optical/IR counterpart is enlightening. It implies that the faintest persistent X-ray sources of the RASS/BSC can be successfully identified with  $1''$  X-ray astrometry using USNO-A2 and 2MASS – that is to say, that successful identification of the RASS/BSC X-ray sources is limited only by confusion, and not by high X-ray/optical flux ratios.

The present approach demonstrates the capability of statistical cross-identification techniques applied using all-sky-surveys (Rutledge et al. 2000). Its advantage over previous approaches of examining individual X-ray sources and their nearby off-band counterparts is that we can “Monte-Carlo” the sky, and quantitatively state selection efficiency for INSs. As such, we are also able to examine the weakness of this approach, and design a superior experiment, which will improve on the present limit.

Improvement on the present limit on the number of INSs requires primarily a more efficient means of statistical identification of INSs, and not substantial numbers of new arcsec localizations of reasonable INS candidates in the RASS/BSC. For example, if we had observed all 32 (spectrally soft) INS candidates with *Chandra*, and there were no new INSs, this would lower the 90% limit from 56 to 34 INSs, an improvement of a factor of  $\sim 1.6$ . However, if our identification efficiency had been 80% instead of 20% but everything else being the same (including having 13 “undetermined” sources), our 90% confidence upper-limit would now be  $<9$  – comparable to the number known – instead of  $<56$ , an improvement of a factor of  $\sim 5.6$ , which would not have required any more observations than we undertook for the present analysis. Thus, efficient statistical identification strategies are more critical to INS identification than are complete observations of “reasonable” candidates. Statistical applications such as this are becoming more common as the Virtual Observatory<sup>6</sup> is developed (NVO Interim Steering Committee 2001), and can be expected to leverage the large all-sky databases with modest new observations, to extract maximum science output.

RER was supported for this work by the *Chandra* Guest Observation program. RER acknowledges stimulating conversations with G. Farrar and L. Bildsten on the subject of

---

<sup>6</sup><http://www.nvosdt.org>

observational limits on the NS birthrate. We are grateful to David Kaplan, Edo Berger and Josh Bloom for obtaining optical images in support of the present work. We are also grateful to the members of the *Chandra* Science Center for production of this exquisite observatory. This research has made use of the NASA/ IPAC Infrared Science Archive, which is operated by the Jet Propulsion Laboratory, California Institute of Technology, under contract with the National Aeronautics and Space Administration. This publication makes use of data products from the Two Micron All Sky Survey, which is a joint project of the University of Massachusetts and the Infrared Processing and Analysis Center/California Institute of Technology, funded by the National Aeronautics and Space Administration and the National Science Foundation. The Digitized Sky Surveys were produced at the Space Telescope Science Institute under U.S. Government grant NAG W-2166. The images of these surveys are based on photographic data obtained using the Oschin Schmidt Telescope on Palomar Mountain and the UK Schmidt Telescope. The plates were processed into the present compressed digital form with the permission of these institutions. The DPOSS project was generously supported by the Norris Foundation.

## References

- Bade, N., Engels, D., Voges, W., Beckmann, V., Boller, T., Cordis, L., Dahlem, M., Englhauser, J., Molthagen, K., Nass, P., Studt, J., & Reimers, D., 1998, *A&AS* 127, 145
- Beuermann, K., Thomas, H.-C., & Pietsch, W., 1991, *A&A* 246, L36
- Blaes, O. & Madau, P., 1993, *ApJ* 403, 690
- Bondi, H., 1952, *MNRAS* 112, 195
- Bondi, H. & Hoyle, F., 1944, *MNRAS* 104, 421
- Colpi, M., Turolla, R., Zane, S., & Treves, A., 1998, *ApJ* 501, 252
- Condon, J. J., Cotton, W. D., Greisen, E. W., Yin, Q. F., Perley, R. A., Taylor, G. B., & Broderick, J. J., 1998, *AJ* 115, 1693
- Cordes, J. M. & Chernoff, D. F., 1998, *ApJ* 505, 315
- Danner, R., 1998a, *A&AS* 128, 331
- Danner, R., 1998b, *A&AS* 128, 349
- de Martino, D., Barcaroli, R., Matt, G., Mouchet, M., Belloni, T., Beuermann, K., Chiappetti, L., Done, C., Gaensicke, B. T., La Franca, F., & Mukai, K., 1998, *A&A* 332, 904
- Dickey, J. M. & Lockman, F. J., 1990, *ARA&A* 28, 215
- Djorgovski, S. G., Gal, R. R., Odewahn, S. C., de Carvalho, R. R., Brunner, R., Longo, G., & Scaramella, R., 1998, in *Wide Field Surveys in Cosmology, 14th IAP meeting held May 26-30, 1998, Paris. Publisher: Editions Frontieres. ISBN: 2-8 6332-241-9, p. 89.*, p. 89
- Dotani, T., Asai, K., & Greiner, J., 1999, *PASJ* 51, 519
- Fischer, J.-U., Hasinger, G., Schwöpe, A. D., Brunner, H., Boller, T., Trümper, J., Voges, W., & Neizvestny, S., 1998, *Astron. Nachr.*, 319, 347-368 (1998) 319, 347
- Fischer, J.-U., Hasinger, G., Schwöpe, A. D., Brunner, H., Boller, T., Trümper, J., Voges, W., Neizvestny, S., Schwarz, R., Ugryumov, A., & Belage, Y., 2002, *VizieR Online Data Catalog* 9032, 0
- Hambaryan, V., Hasinger, G., Schwöpe, A. D., & Schulz, N. S., 2002, *A&A* 381, 98
- Hansen, B. M. S. & Phinney, E. S., 1997, *MNRAS* 291, 569
- Hawley, S. L., Covey, K. R., Knapp, G. R., Golimowski, D. A., Fan, X., Anderson, S. F., Gunn, J. E., Harris, H. C., Ivezić, Ž., Long, G. M., Lupton, R. H., McGehee, P. M., Narayanan, V., Peng, E., Schlegel, D., Schneider, D. P., Spahn, E. Y., Strauss, M. A., Szkody, P., Tsvetanov, Z., Walkowicz, L. M., Brinkmann, J., Harvanek, M., Hennessy, G. S., Kleinman, S. J., Krzesinski, J., Long, D., Neilsen, E. H., Newman, P. R., Nitta, A., Snedden, S. A., & York, D. G., 2002, *AJ* 123, 3409
- Kaplan, D. L., Kulkarni, S. R., & van Kerkwijk, M. H., 2002, *ApJ* 579, L29
- Kulkarni, S. R. & van Kerkwijk, M. H., 1998, *ApJ* 507, L49

- Li, J. Z., Hu, J. Y., & Chen, W. P., 2000, *A&A* 356, 157
- Lorimer, D. R., Bailes, M., & Harrison, P. A., 1997, *MNRAS* 289, 592
- Madau, P. & Blaes, O., 1994, *ApJ* 423, 748
- Marino, A., Micela, G., & Peres, G., 2000, *A&A* 353, 177
- Motch, C., Guillout, P., Haberl, F., Pakull, M., Pietsch, W., & Reinsch, K., 1997a, *A&A* 318, 111
- Motch, C., Guillout, P., Haberl, F., Pakull, M. W., Peitsch, W., & Reinsch, K., 1997b, *A&AS* 122, 201
- Motch, C., Haberl, F., Zickgraf, F.-J., Hasinger, G., & Schwope, A. D., 1999, *A&A* 351, 177
- Neuhäuser, R. & Trümper, J. E., 1999, *A&A* 343, 151
- NVO Interim Steering Committee, 2001, in R. J. Brunner, S. G. Djorgovski, & A. S. Szalay (eds.), *ASP Conf. Ser. 255: Virtual Observatories of the Future*, p. 353, astro-ph/0108115
- Popov, S. B., Colpi, M., Prokhorov, M. E., Treves, A., & Turolla, R., 2000a, *ApJ* 544, L53
- Popov, S. B., Colpi, M., Treves, A., Turolla, R., Lipunov, V. M., & Prokhorov, M. E., 2000b, *ApJ* 530, 896
- Press, W., Flannery, B., Teukolsky, S., & Vetterling, W., 1995, *Numerical Recipes in C*, Cambridge University Press
- Rutledge, R. E., 2001, *ApJ* 553, 796
- Rutledge, R. E., Brunner, R. J., Prince, T. A., & Lonsdale, C., 2000, *ApJS* 131, 335
- Schwope, A., Hasinger, G., Lehmann, I., Schwarz, R., Brunner, H., Neizvestny, S., Ugryumov, A., Balega, Y., Trümper, J., & Voges, W., 2000a, *Astronomische Nachrichten, vol. 321, no. 1, p. 1-52.* 321, 1
- Schwope, A., Hasinger, G., Lehmann, I., Schwarz, R., Brunner, H., Neizvestny, S., Ugryumov, A., Balega, Y., Trümper, J., & Voges, W., 2000b, *Astronomische Nachrichten* 321, 1
- Singh, K. P., Szkody, P., Barrett, P., White, N. E., Fierce, E., Silber, A., Hoard, D. W., Hakala, P. J., Piirola, V., & Sohl, K., 1995, *ApJ* 453, L95+
- Szkody, P., Anderson, S. F., Agüeros, M., Covarrubias, R., Bentz, M., Hawley, S., Margon, B., Voges, W., Henden, A., Knapp, G. R., Vanden Berk, D. E., Rest, A., Miknaitis, G., Magnier, E., Brinkmann, J., Csabai, I., Harvanek, M., Hindsley, R., Hennessy, G., Ivezic, Z., Kleinman, S. J., Lamb, D. Q., Long, D., Newman, P. R., Neilsen, E. H., Nichol, R. C., Nitta, A., Schneider, D. P., Snedden, S. A., & York, D. G., 2002, *AJ* 123, 430
- Thomas, H. C., Beuermann, K., Reinsch, K., Schwope, A. D., Truemper, J., & Voges, W., 1998, *A&A* 335, 467
- Toropina, O. D., Romanova, M. M., Toropin, Y. M., & Lovelace, R. V. E., 2001, *ApJ* 561,

964

- Treves, A. & Colpi, M., 1991, *A&A* 241, 107
- Treves, A., Turolla, R., Zane, S., & Colpi, M., 2000, *PASP* 112, 297
- van Dokkum, P. G., 2001, *PASP* 113, 1420
- Voges, W., Aschenbach, B., Boller, T., Bräuninger, H., Briel, U., Burkert, W., Dennerl, K., Englhauser, J., Gruber, R., Haberl, F., Hartner, G., Hasinger, G., Kürster, M., Pfeffermann, E., Pietsch, W., Predehl, P., Rosso, C., Schmitt, J. H. M. M., Truemper, J., & Zimmermann, H. U., 1999, *A&A* 349, 389
- Walter, F. M. & Matthews, L. D., 1997, *Nature* 389, 358
- Watson, M. G., King, A. R., & Williams, G. A., 1987, *MNRAS* 226, 867
- White, N., Giommi, P., & Angelini, L., 1994, Paper presented at the HEAD Meeting of the AAS; November 1994, <http://lheawww.gsfc.nasa.gov/users/white/wgacat/head.html>
- Yakovlev, D. G., Kaminker, A. D., & Gnedin, O. Y., 2001, *A&A* 379, L5
- Zampieri, L., Campana, S., Turolla, R., Chierigato, M., Falomo, R., Fugazza, D., Moretti, A., & Treves, A., 2001, *A&A* 378, L5
- Zickgraf, F. J., Thiering, I., Krautter, J., Appenzeller, I., Kneer, R., Voges, W. H., Ziegler, B., Chavarria, C., Serrano, A., Mujica, R., Pakull, M., & Heidt, J., 1997, *A&AS* 123, 103
- Zombeck, M. V., 1982, *Handbook of space astronomy and astrophysics*, Cambridge, Cambridge University Press



Fig. 1.— **(a)** Distribution in Galactic Coordinates of the 150 control fields. These objects mimic INs, in that they will have no detectable off-band counterparts in the USNO-A2, IRAS, or NVSS catalogs. **(b)** Distribution in Galactic Coordinates of the 29 (of 150) control fields with  $P_{\text{no-id}} > 0.90$ . These largely avoid the plane, where the source density produces many (low significance) candidate associations. **(c)** The distribution of  $P_{\text{id}}$  values for optical sources in the 150 control fields. The vast majority are of low significance, as expected for spurious associations. However, when  $\gtrsim$  few of these appear in the same control field, as occurs in the Galactic plane, the sum of the  $P_{\text{id}}$  values removes the X-ray sources from our selection. **(d)** The cumulative distribution  $N(< |b|)$  of the 29 control fields with  $P_{\text{no-id}} > 0.90$  (solid line) compared with an equal number per sky-area distribution (dotted line). The observed distribution is discrepant from the equal area distribution (the probability of producing the observed distribution from the theoretical distribution is  $3 \times 10^{-6}$ ) due to the effects of confusion in the Galactic plane.

Fig. 2.— R-band 5-min ESI image taken at Keck II on 2002 Nov 5 UT, of the field of 1RXS J0203-3438. Cosmic rays were removed by application of the “L.A.COSMIC” algorithm (van Dokkum 2001). North is up, east to the left. The intensity gradient across the field is due to a bright optical source which is  $1.5'$  off-image. The localization of the *Chandra* X-ray source is indicated by the cross, with a  $0.6''$  ( $2\sigma$ ) positional uncertainty. For this figure, relative astrometry was performed with a second X-ray source detected in the HRC image, which is coincident with a bright DSS source, and is also detected as a point source ( $0.8''$  seeing) in the ESI image. The *Chandra* source is spatially associated with an optical point source, with two nebulosities to the north-east and to the north.

Fig. 3.— Field of 1RXS J1328–3554, from UK Schmidt 48-inch survey (left panel, Epoch 1975.27), second epoch survey UKSTU Schmidt survey (center panel, Epoch 1991.2), and 2MASS *J*-band image (right panel, Epoch 1999.45, scaled logarithmically in intensity). Hash marks denote the localization of the *Chandra* X-ray source. Circles mark the positions of the 2MASS IR sources found in the field. The epoch of the *Chandra* observation is 2001.2. The *Chandra* source is coincident with a red, apparent high proper motion object ( $\sim 165$  mas/yr), which we interpret as a nearby low-mass star.

Fig. 4.— DPOSS g-band image of the field of 1RXS J1450+6559. The large circle is the  $3\sigma$  RASS localization. The small (black) circle is the  $1''$  *Chandra* positional uncertainty. The optical source coincident with the *Chandra* position is fainter than the DSS plate limit, and so not included in the USNO-A2 catalog.

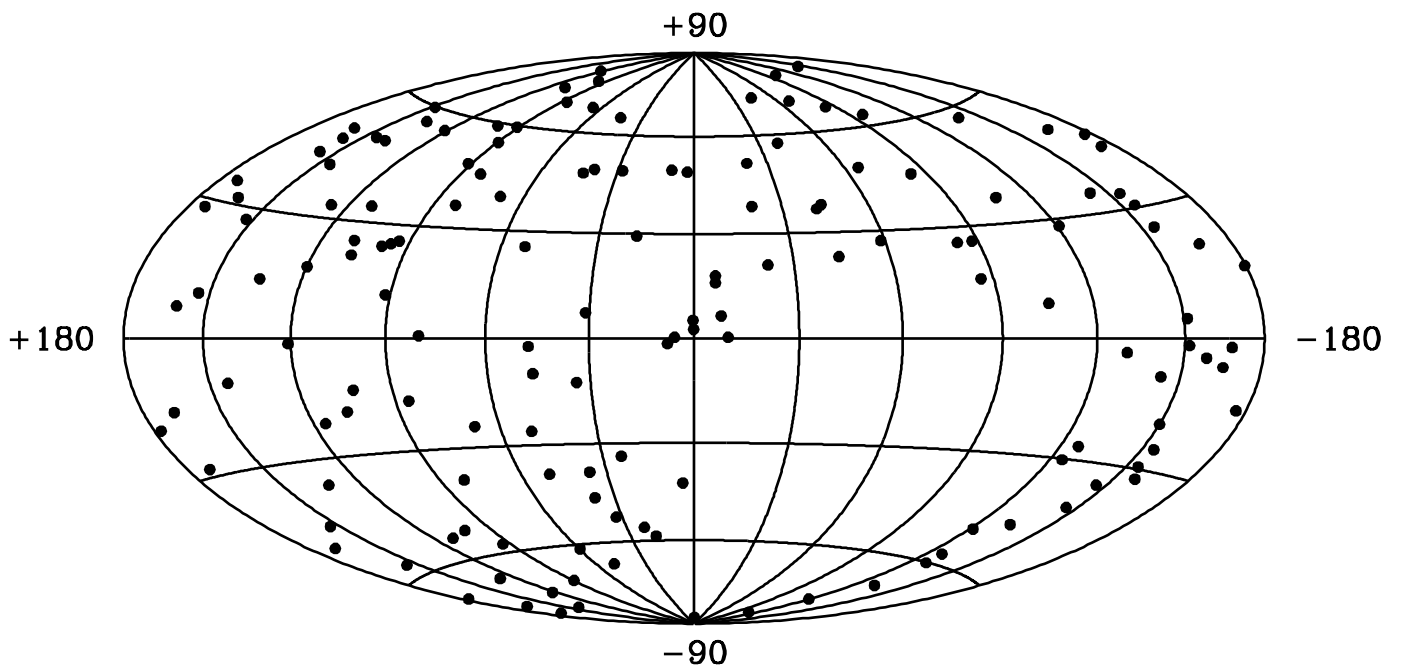
Fig. 5.— KECK/LRIS optical spectra (not flux calibrated) of proposed optical counterparts. **Top Panel:** 1RXS J1450+6559 contains three prominent emission lines at  $6555\text{\AA}$ ,  $6668\text{\AA}$ , and  $7055\text{\AA}$ . Absorption features at  $6862$ ,  $7180$ ,  $7234$ ,  $7596$ , and  $7621\text{\AA}$  are sky lines. **Center Panel:** 1RXS J1639+5656 shows one prominent broad emission line, at  $7412\text{\AA}$ . The absorption features (in particular, those at  $7233$ ,  $7267\text{\AA}$  and  $7595$ ,  $7625\text{\AA}$ ) are due to imperfect sky subtraction. **Bottom Panel:** Sky spectrum.

Fig. 6.— DPOSS g-band image of field 1RXS J1639+5656. The large circle is the  $42''$  ( $3\sigma$ ) RASS/BSC localization uncertainty; the small (black) circle, indicated by the hash marks, is the  $1''$  radius *Chandra* localization, which is positionally coincident with an extended source, an apparent AGN at  $z = 1.65$ .

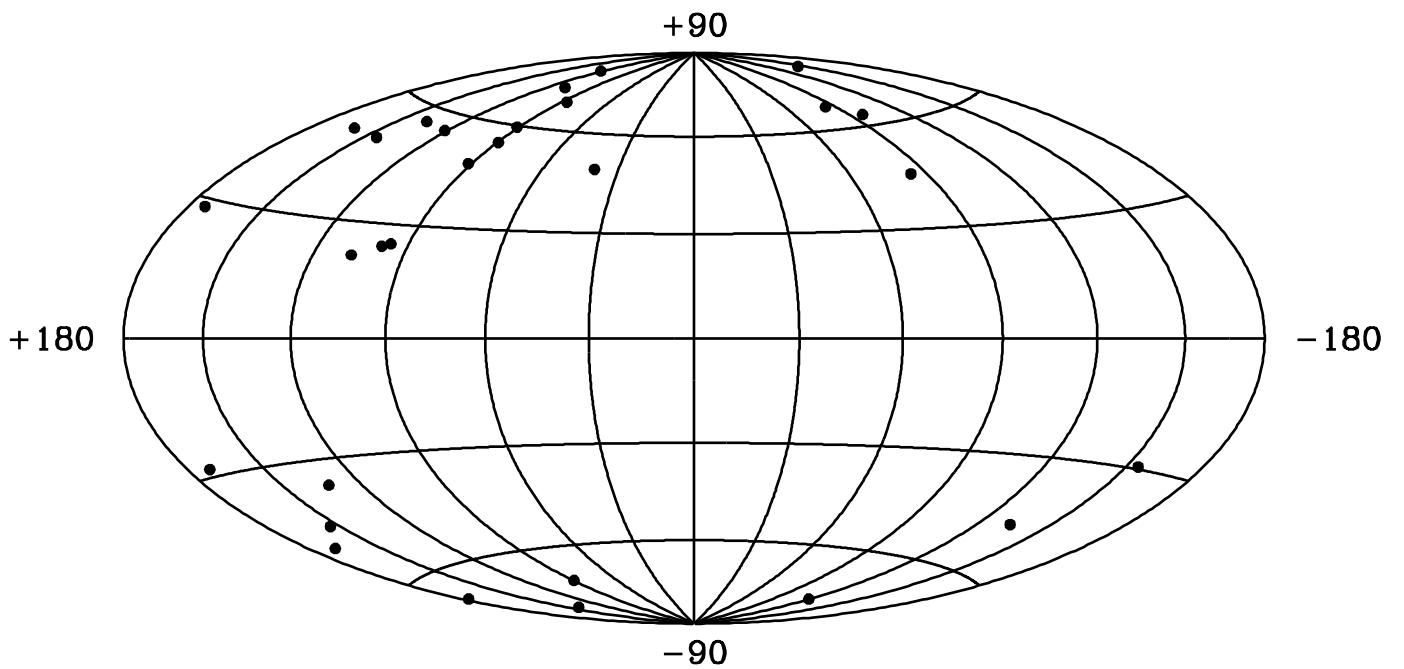
Fig. 7.— DSS fields of the 8 candidate INSs observed with *Chandra*. The large circle is the  $3\sigma$  RASS/BSC positional uncertainty, labeled with the RASS source name. Those with X-ray sources detected with *Chandra* have a cross, representing the  $1''$  *Chandra* positional uncertainty, labeled with the *Chandra* source name. In the upper-right corner, we give the Galactic coordinates (deg) of the X-ray source, and the equivalent Hydrogen column density ( $N_{\text{H}}$ ) in units of  $\text{cm}^{-2}$ . In the lower-left corner, we list  $P_{\text{id}}$ , the probability the RASS/BSC source is associated with one of the off-band sources; USNO-A2 sources which individually have a non-zero probability of being associated with the RASS/BSC source are labeled with their individual  $P_{\text{id}}$  value. We also list in the lower-left corner the RASS/BSC hardness ratio (HR1) and PSPC countrate. (see more discussion in text).

Fig. 8.— Probability distribution  $P_{\text{XID}}(p)$ , where  $p$  is the probability that an INS in our survey field is found by our statistical-identification procedure.

Fig. 9.— The probability distribution  $P_{\text{BG}}$  (Eq. 8) that there are  $N$  INSs in our selection of 32, yet end up with only 2 INSs in the 15 following the removal of 17 from our sample due to associated optical sources in the field. Here,  $N_{\text{INS},\text{min}} = 2$ ,  $T = 32$ ,  $BG = 17$ .



All Control Sources (150/150)



Control Sources (29/150),  $P_{\text{no-id}} > 0.90$

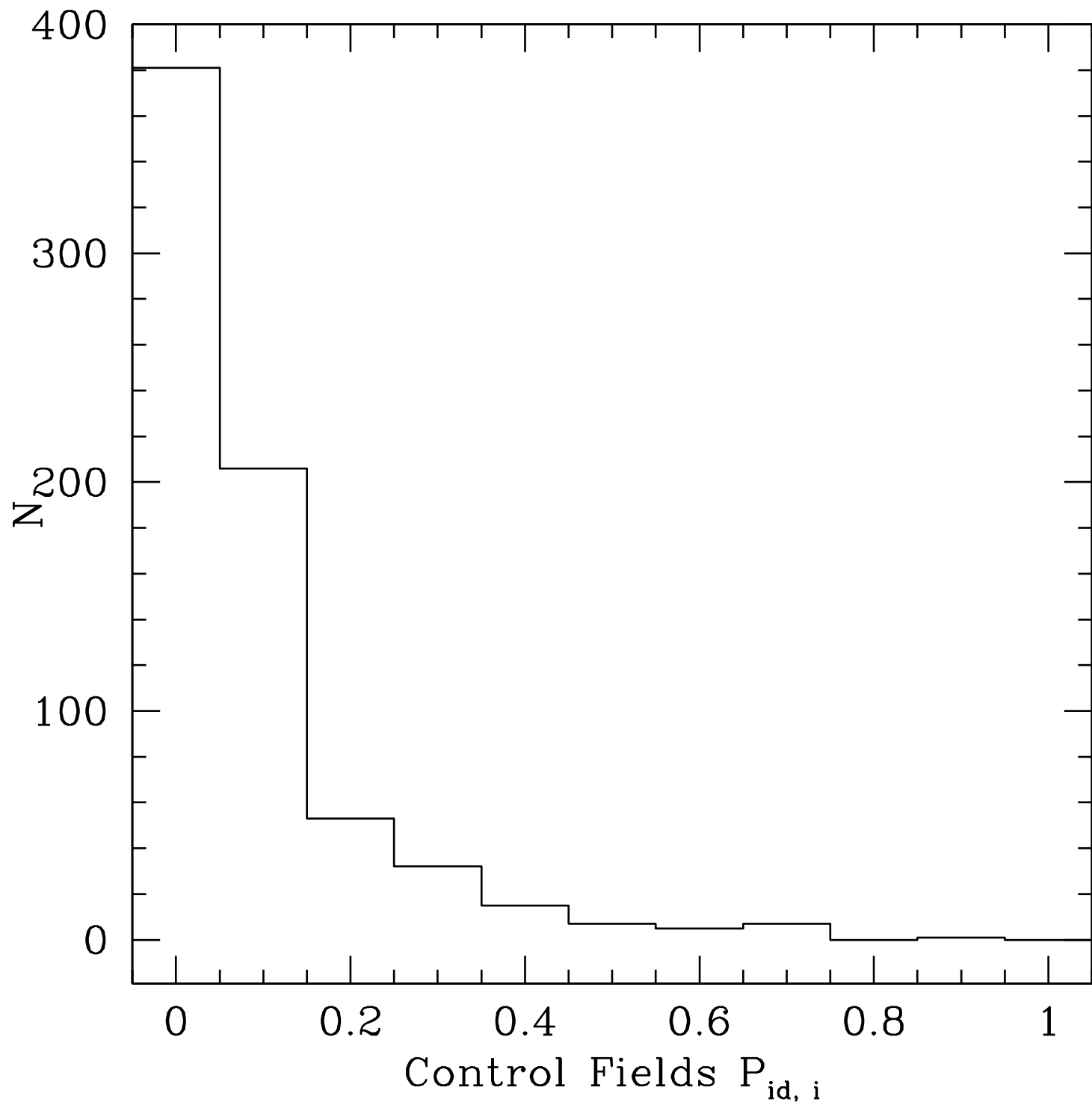


Figure 1c

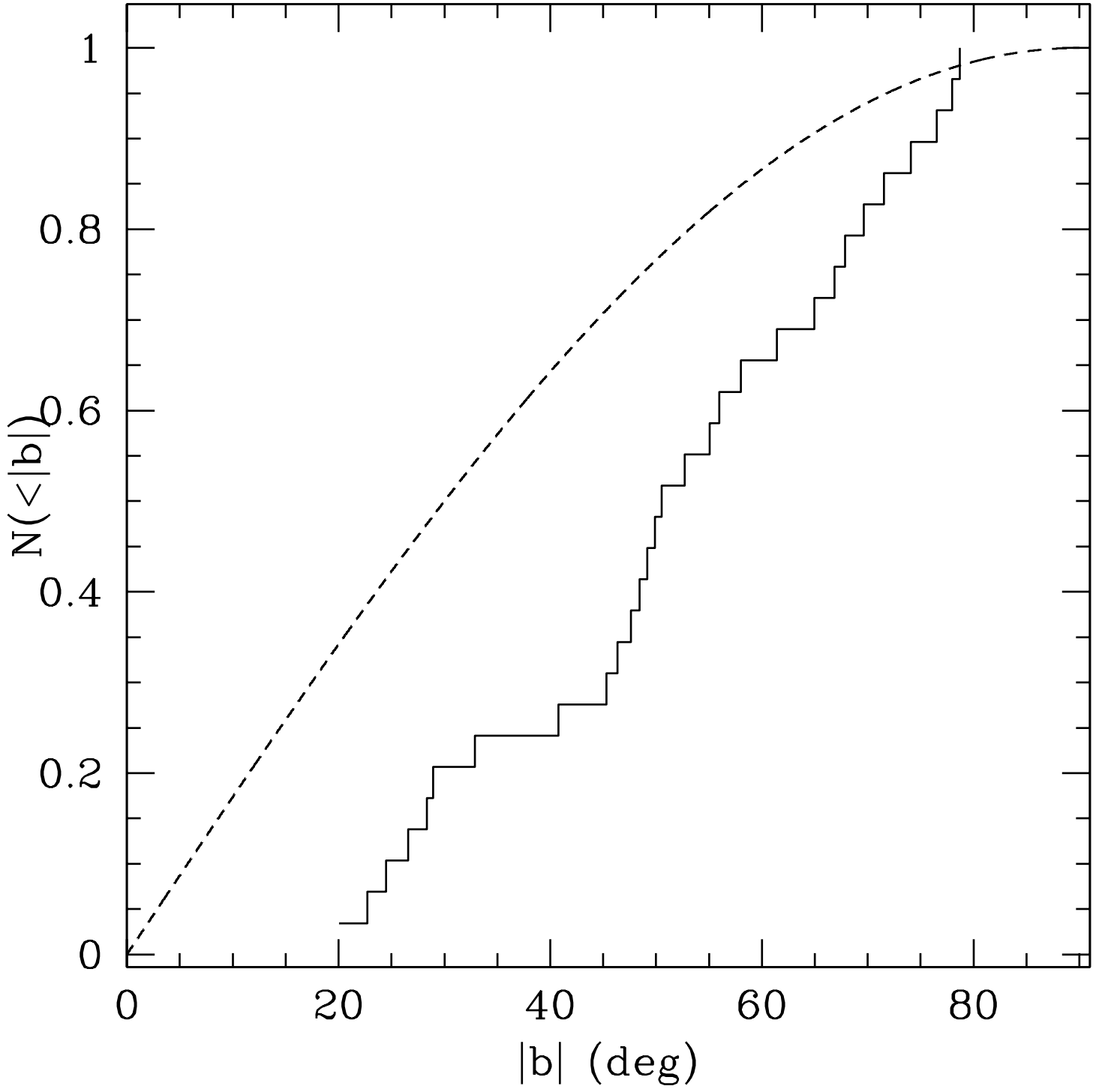


Figure 1d

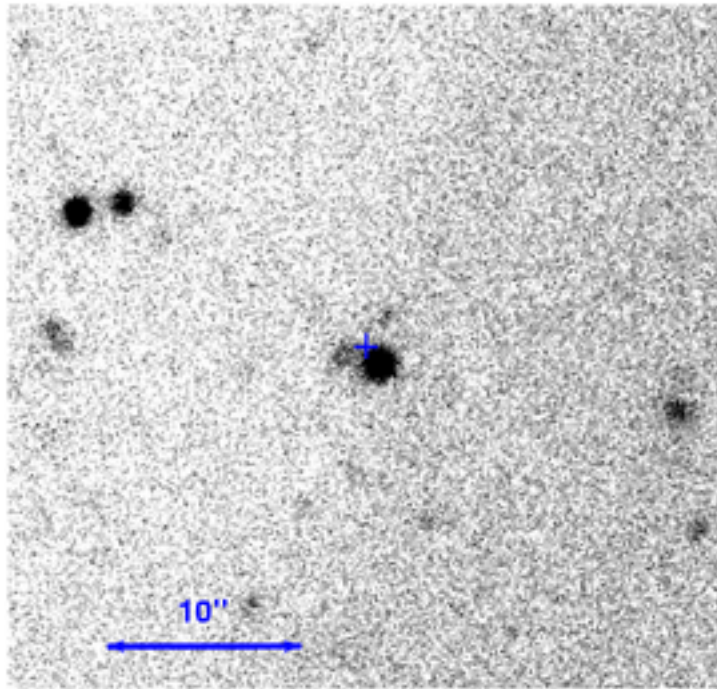


Figure 2



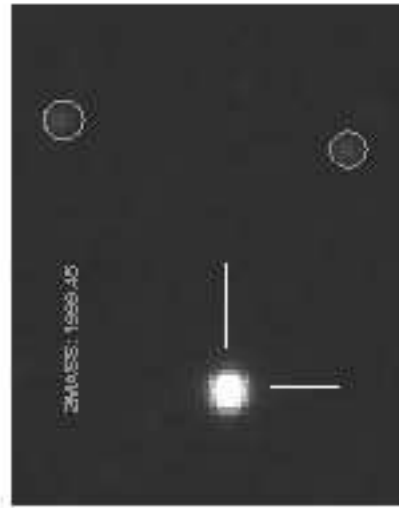


Figure 3

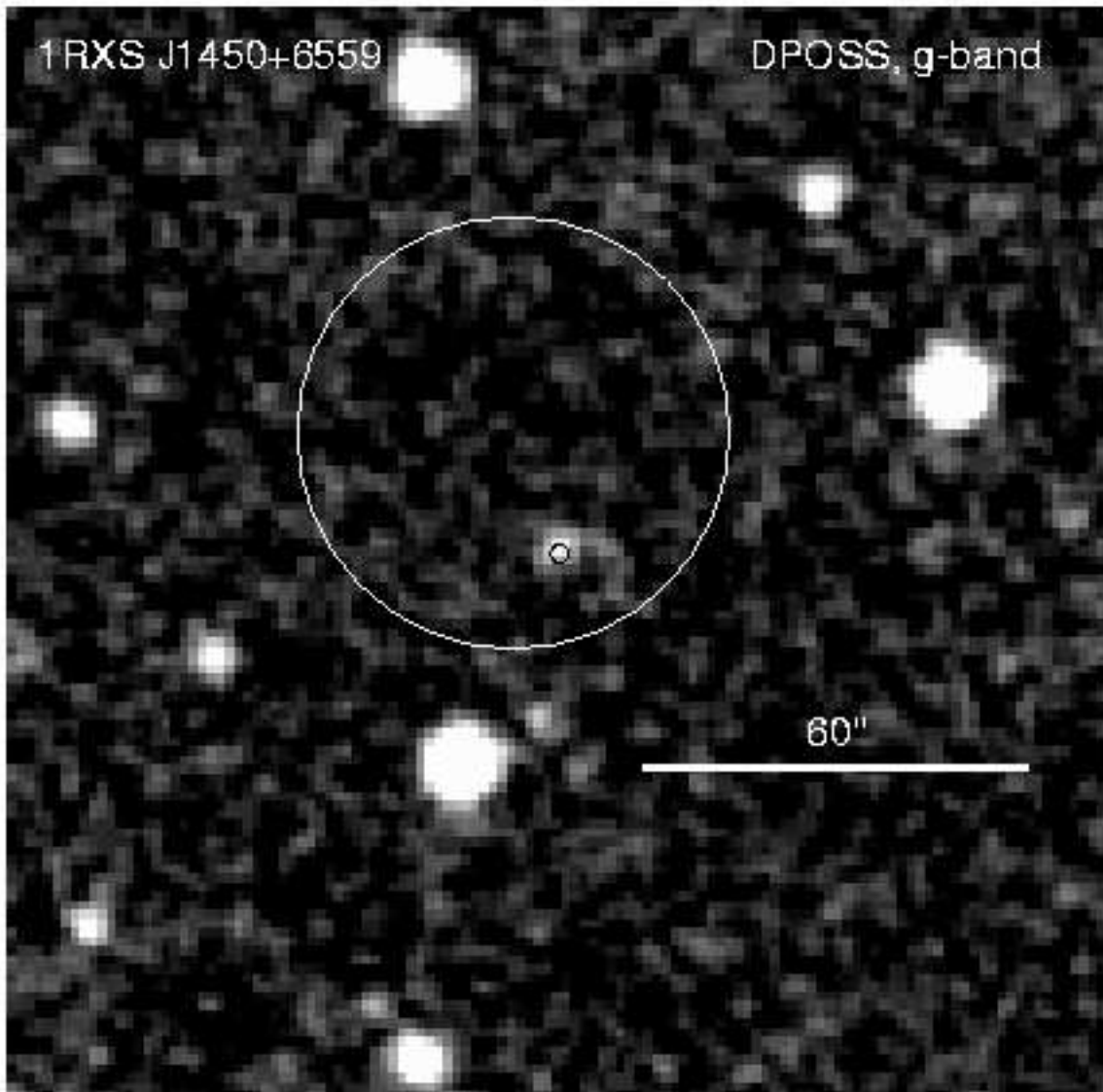


Figure 4

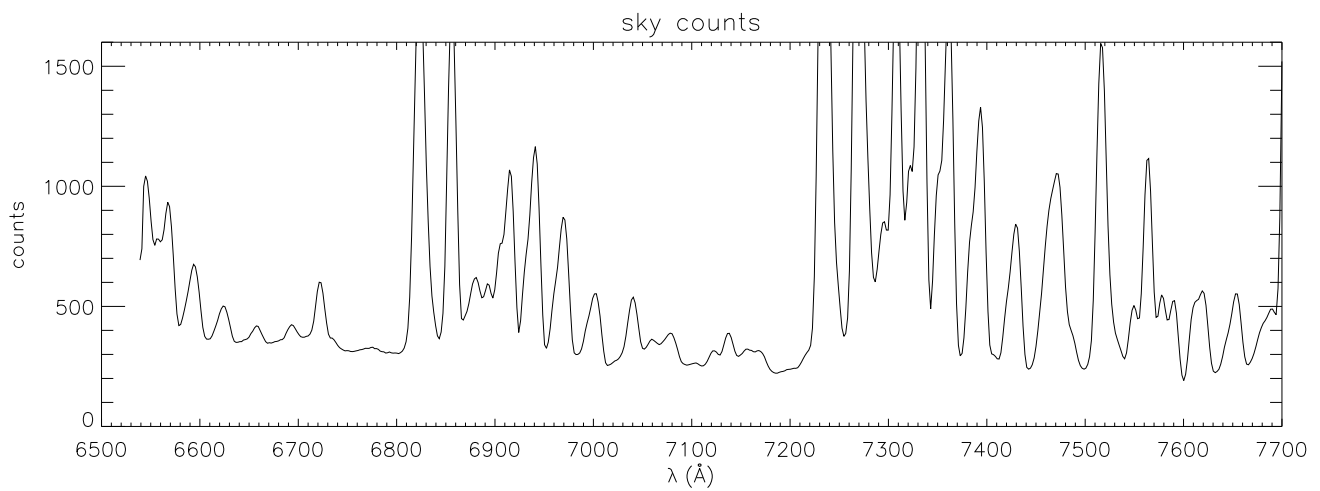
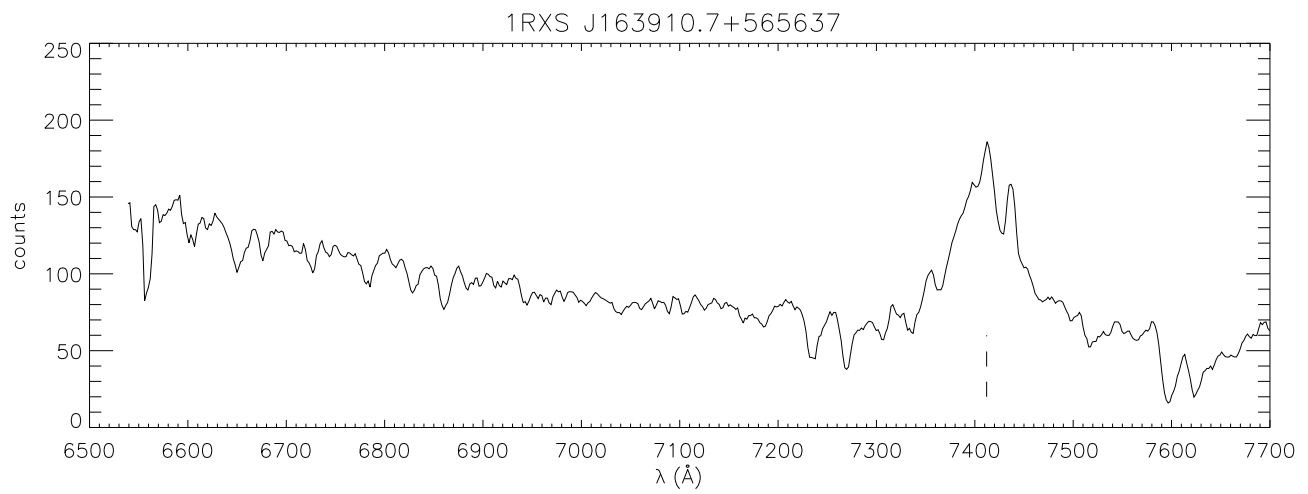
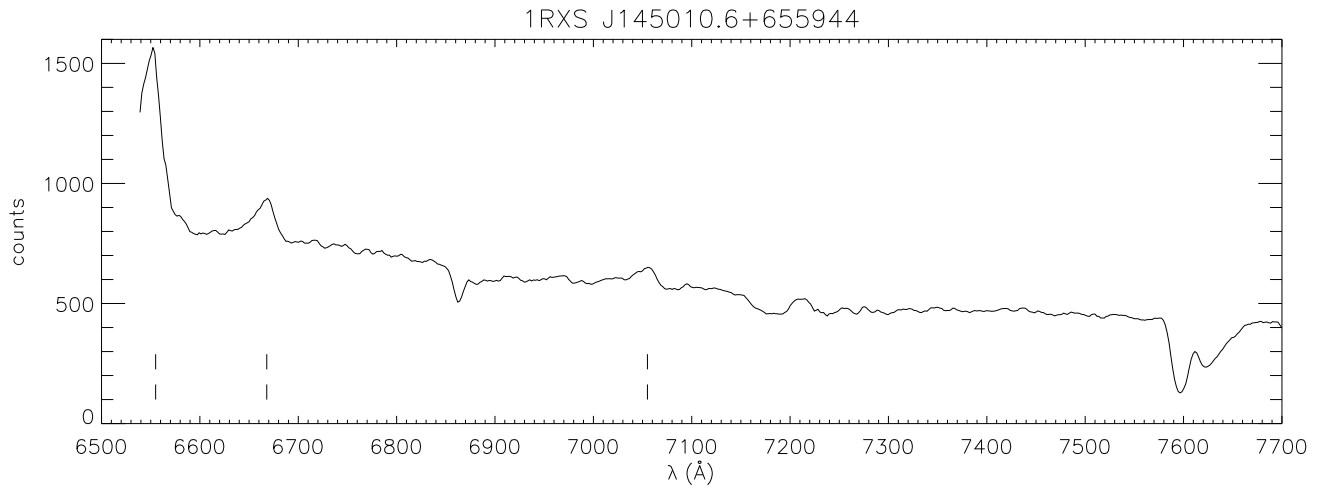


Figure 5

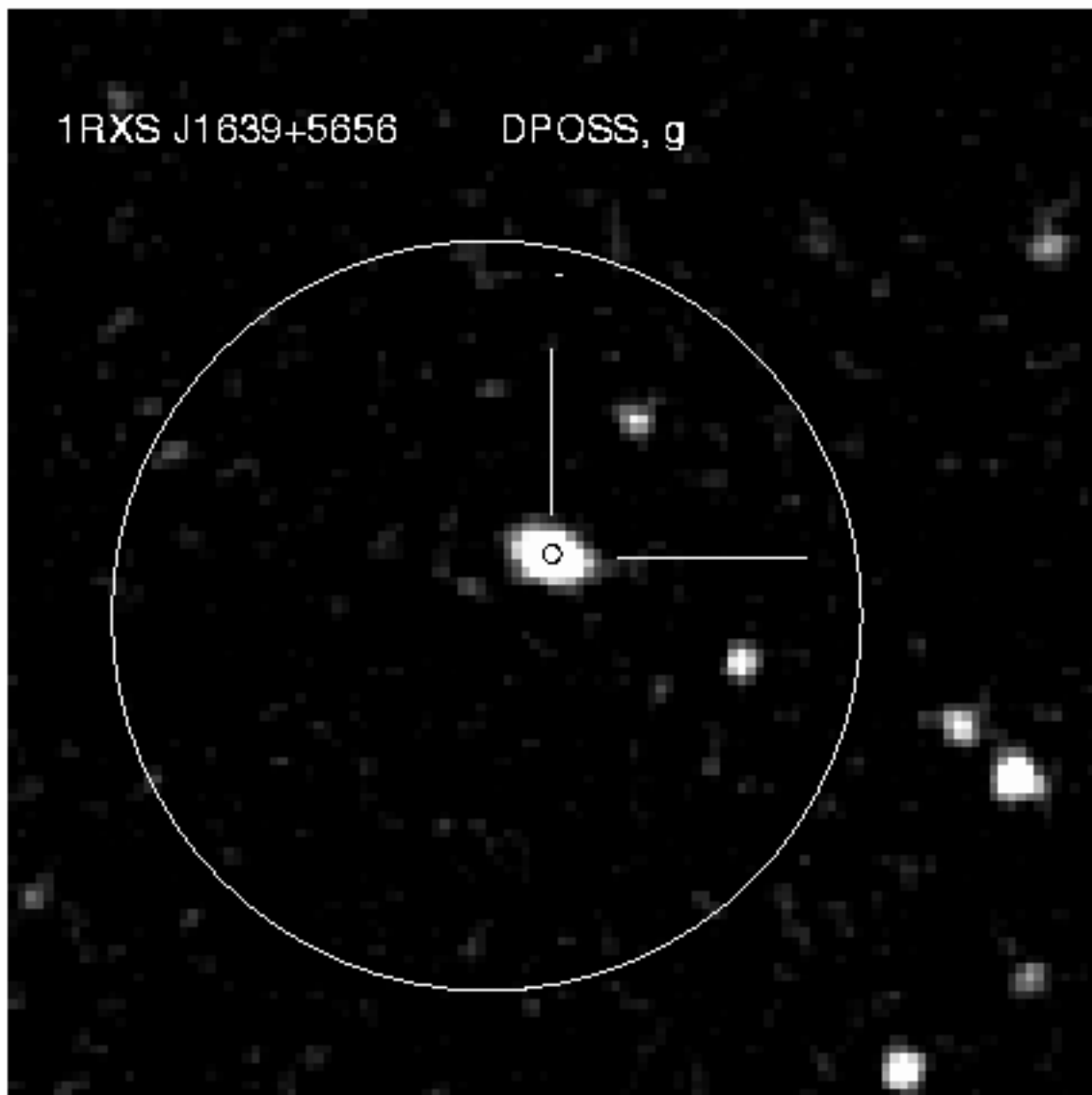


Figure 6

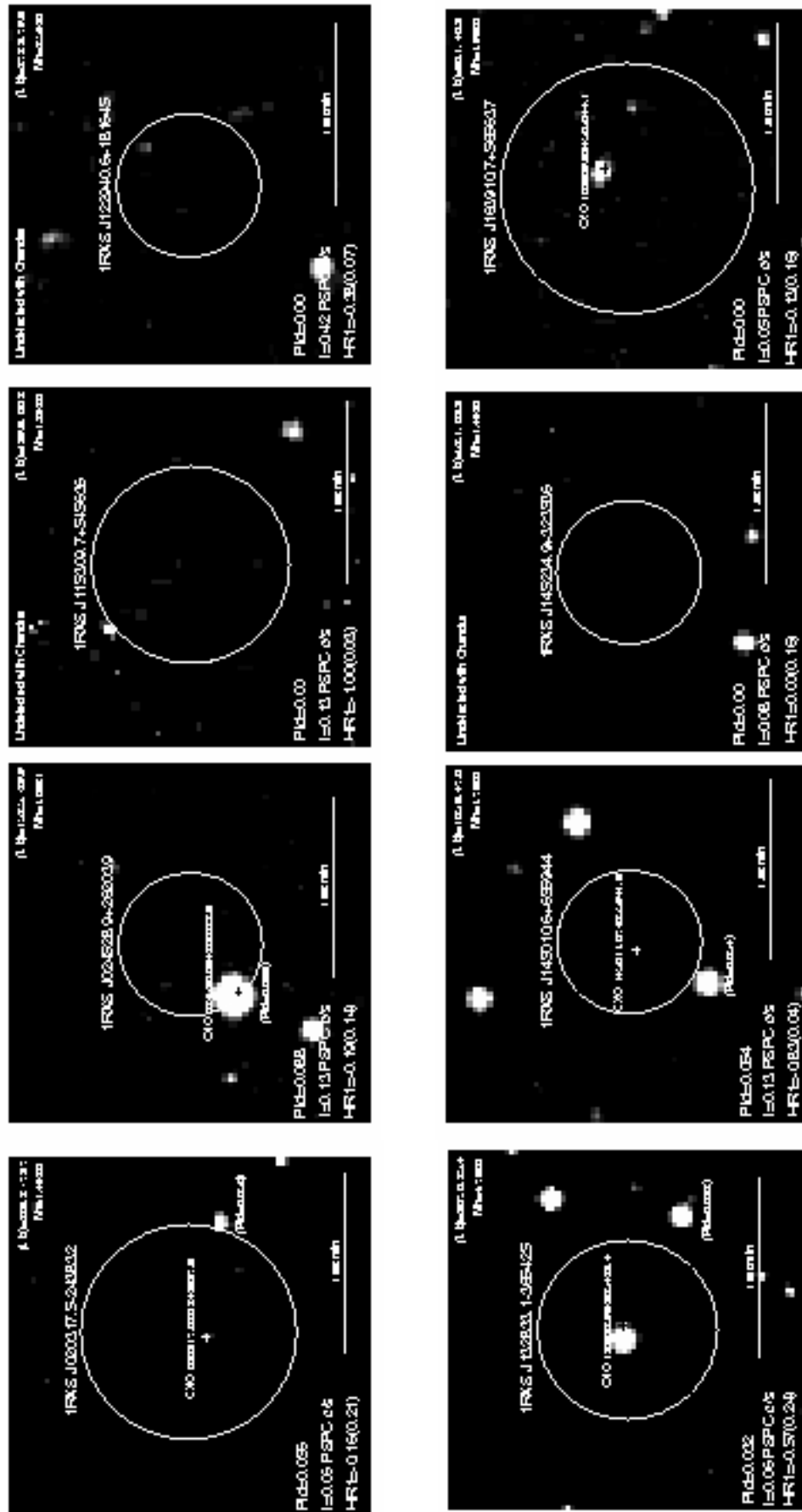


Figure 7

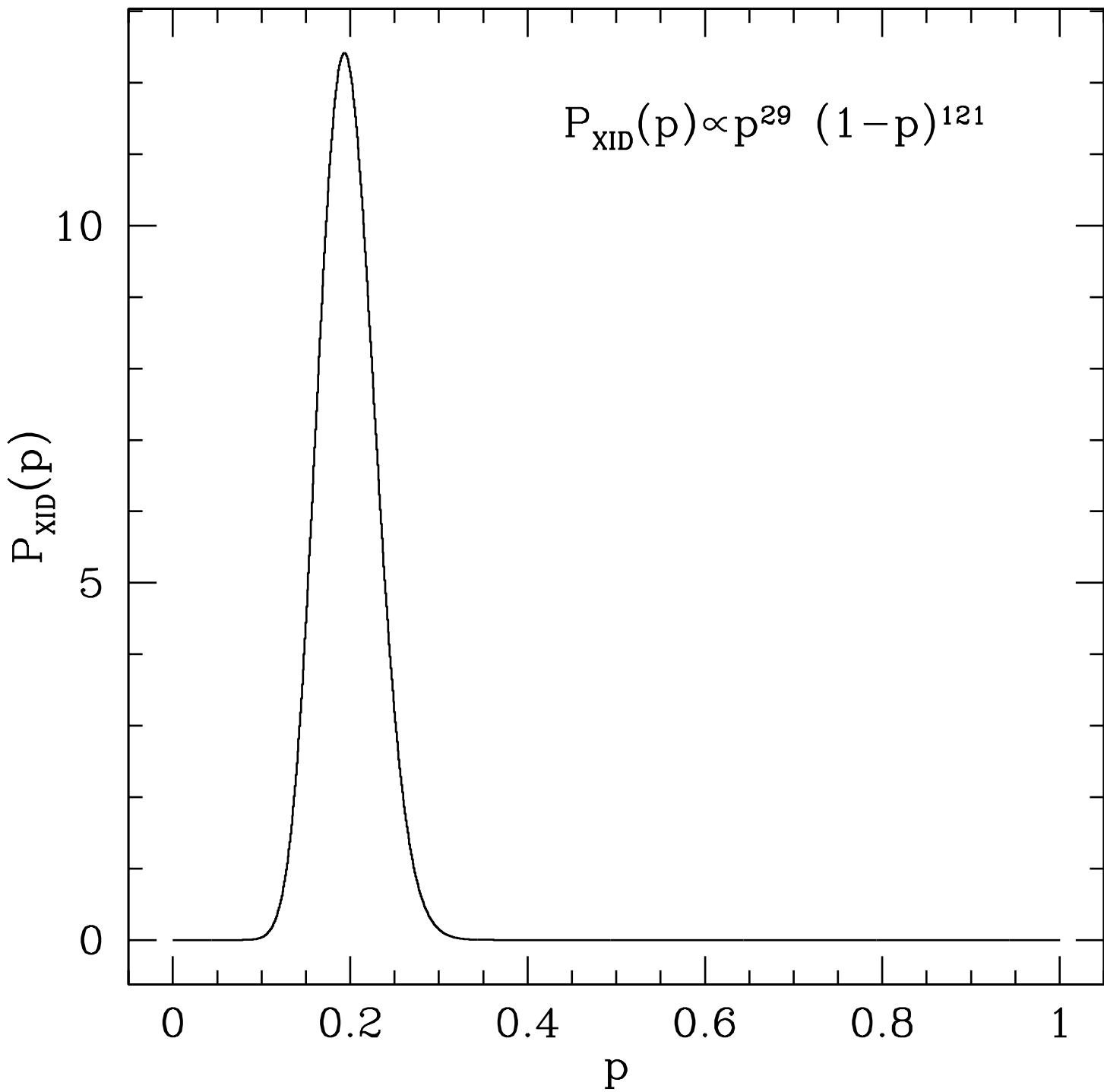


Figure 8

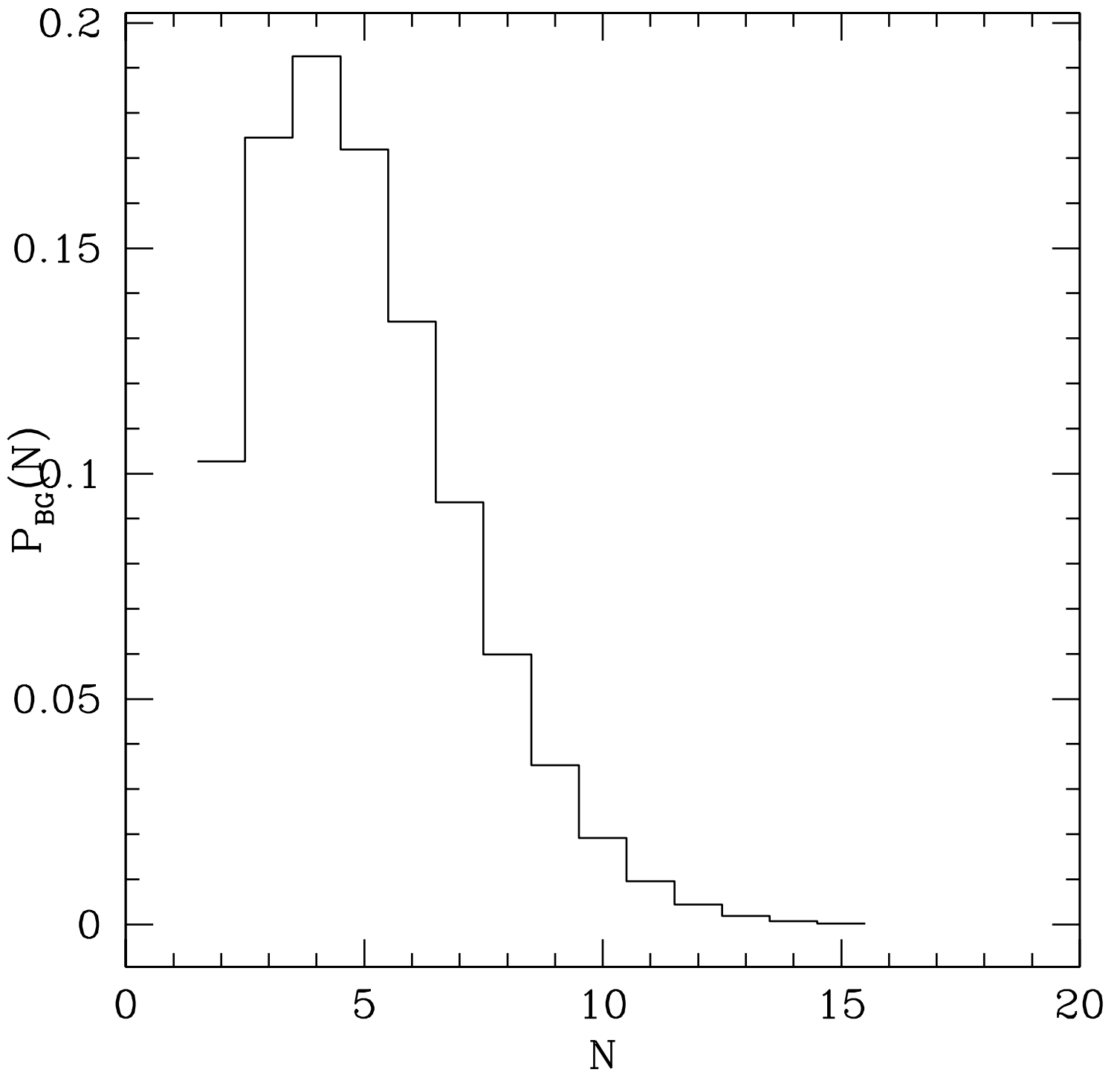


Figure 9

Table 1. Identified INSs

INS	$1-P_{\text{no-id}}$	High $P_{\text{id}}$ Object <sup>a</sup>
MS 0317.7–6647	n/a	n/a
RX J185635–3754	0.89	$B=17.4; r=6.7''$
RX J0720.4–3125	1.0	$B=20.2, r = 6.4''$
RX J0420.0–522	n/a	n/a
RX J1308.6+2127	0.0	no sources
RX J1605.3+3249	0.0	no sources
RX J0806.4–4132	n/a	n/a
RX J2143.0+0654	0.89	$B = 19.4, r = 22.4''$

Note. — X-ray sources classified as INSs (Treves et al.2000; Zampieri et al. 2001) n/a = Not included in our analysis (either at  $\delta < -39$  or not in RASS/BSC).

<sup>a</sup> The single object which has the highest probability of association.



Table 2. Table of Thirty Two INS Candidates

1RXS J	RBS #	type	Name	<i>Chandra</i> /HRI Obs.?	INS?	ID. Ref.
020146.5+011717	269	*	...	...	undetermined	
020317.5-243832		AGN	CXO J020317.62-243837.8	<i>Chandra</i>	not an INS	(§ 4.1)
024946.0-382540		...	...	...	undetermined	
024528.9+262039		*	...	<i>Chandra</i>	not an INS	(§ 4.1)
031413.7-223533		nova/star	EF Eri	...	not an INS	1,2
032620.8+113106		T-Tauri	...	...	undetermined	3
041215.8+644407		Fl*	G 247-15	...	undetermined	10
043334.8+204437		Fl*	G 8-41	...	undetermined	10
051541.7+010528		CV/AM-Her	V* V1309 Ori	...	not an INS	4
051723.3-352152		MV:e	EUVE J0517-35.3	...	undetermined	
075556.7+832310		Fl*	EUVE J0755+83.3	...	undetermined	10
091010.2+481317		Sy1	QSO B0906+484	...	undetermined	
094432.8+573544		AGN	DPOSS 094432.42+573534.9	<i>ROSAT</i> /HRI	not an INS	(§ 4.2)
104710.3+633522		CV/DQ Her	V* FH Uma	...	not an INS	5
115309.7+545636		...	...	<i>Chandra</i>	not an INS	(§ 4.1)
122940.6+181645	1116	BL-Lac	...	<i>Chandra</i>	not an INS	(§ 4.1)
123319.0+090110		**	GJ 473B	...	not an INS	6
125015.2+192357		Sy1	...	...	undetermined	
130034.2+054111		Fl*	V* FN Vir	...	undetermined	
130402.8+353316		QSO	QSO B1301+358	...	undetermined	
130547.2+641252		...	...	<i>ROSAT</i> /HRI	not an INS	(§ 4.2)
130753.6+535137	1219	CV/AM-Her	V* EV UMa	<i>ROSAT</i> /HRI	not an INS	(§ 4.2)
130848.6+212708	1223	INS	...	...	INS	7
132833.1-365425		HiPM*	CXO J132832.98-365423.4	<i>Chandra</i>	not an INS	(§ 4.1)
134210.2+282250	1306	CV in M3	...	...	not an INS	8
145010.6+655944		CV	...	<i>Chandra</i>	not an INS	(§ 4.1)
145234.9+323536		...	...	<i>Chandra</i>	not an INS	(§ 4.1)
160518.8+324907	1556	INS	...	...	INS	9
163421.2+570933		HiPM**	2MASS J163420.44+570944.0	<i>ROSAT</i> /HRI	not an INS	(§ 4.2)
163910.7+565637		AGN	CXO J163909.83+565644.1	<i>Chandra</i>	not an INS	(§ 4.1)
231543.7-122159	1970	HiPM*	L 863-30	...	undetermined	
231728.9+193651	1978	Fl*	G 68-5	...	undetermined	

Note. — =bright ( $V < 15$ ) source in DSS, but not cataloged in USNO-A2, within  $30''$  of RASS/BSC position. not an INS=Definitively not an INS. INS= Previously identified as an INS. \*=star; Fl\*=flare star; HiPM\*=high proper-motion star; HiPM\*\*=high proper-motion binary; undetermined=X-ray source which has not been definitively excluded as an INS. Refs: 1, Watson et al. (1987); 2, Beuermann et al. (1991); 3, Li et al. (2000); 4, de Martino et al. (1998); 5, Singh et al. (1995); 6, Marino et al. (2000); 7, Hambaryan et al. (2002); 8, Dotani et al. (1999); 9, Motch et al. (1999); 10, this work.

Table 3. INs Candidate Source and *Chandra* Observation List

1RXS J	$P_{\text{no-id}}$	PSPC c/s	HR1 ( $\pm$ ) <sup>a</sup>	RASS $1\sigma$ (arcsec)	<i>Chandra</i> ObsID	Obs. Start (TT)	Dur. (sec)
0203–2438	0.94	0.06	-0.16 (0.21)	12	1973	2001 Jan 28 11:19	910
0245+2620	0.91	0.13	-0.19 (0.14)	8	1974	2001 Jan 16 03:06	821
1153+5456	1.0	0.13	-1.00 (0.03)	11	1975	2001 Nov 19 22:54	846
1229+1816	1.0	0.42	-0.38 (0.07)	8	1976	2001 Mar 24 04:46	1124
1328–3654	0.96	0.06	-0.57 (0.24)	10	1977	2001 Mar 24 06:40	1325
1450+6559	0.95	0.13	-0.83 (0.04)	8	1978	2001 Sep 07 17:33	823
1452+3235	1.0	0.08	0.00 (0.16)	8	1979	2001 Mar 24 05:25	1334
1639+5656	1.0	0.05	-0.13 (0.16)	14	1980	2001 Sep 07 18:10	1172

Note. — <sup>a</sup>. HR1 is a hardness ratio (see text), for which HR1=0.0 corresponds to 200 eV, and lower values are <200 eV.

 Table 4. *Chandra* and ROSAT/HRI X-ray Source Localizations and Classifications

1RXS J	predicted I <sup>a</sup> (c/ksec)	observed I (c/ksec)	Source Position R.A./dec. (J2000)	Notes
0203–2438	70	35(6)	CXO J020317.626–243837.8	AGN?
0245+2620	140	41(7)	CXO J024530.08+262022.8	M3-star
1153+5456	30	$\leq 4.7$	undetected	n/a
1229+1816	400	$\leq 2.7$	undetected	n/a
1328–3654	50	687(25)	CXO J132832.98–365423.4	proper-motion star
1450+6559	50	62(8)	CXO J145011.07+655941.8	LRIS spectrum; CV
1452+3235	100	$\leq 2.3$	undetected	n/a
1639+5656	50	47(6)	CXO 163909.83+565644.1	extended, LRIS spectrum; AGN
0944+5735	45	9(1)	1RXH J094431.8+573538	AGN?
1305+6412	55	$< 3$	undetected	n/a
1307+5351	600	$< 0.5$	undetected	CV
1634+5709	55	38(4)	1RXH J163421.2+570941	High proper-motion binary

Note. — <sup>a</sup>. Predicted countrate, based on spectral hardness and *ROSAT*/PSPC countrate. Count-rate upper limits are not formally detection limits, but limits on the average countrate. Nominal positional uncertainties for blind pointing of *Chandra* are  $1''$ . The positional uncertainty for CXO J020317.626–243837.8 is  $0.4''$  due to a second X-ray source detected in the HRC image.

Table 5. Off-band Catalog Detections at  $\sim$ arcsec Localizations

CXO	2MASS (quicklook)	2MASS (catalog)	DPOSS
CXO 020317.60–243839.5	no	...	...
CXO 024530.08+262022.8	yes	0245300+262023 ( $J, H, K$ )=9.45(3),8.73(3),8.58(3)	024530.10+262021.3 ( $g, r, i$ )=14.24,13.54,sat.
CXO 132832.98–365423.4	yes	...	...
CXO 145011.07+655941.8	no	...	145011.13+655941.7 ( $g, r, i$ )=19.49,20.09,19.00
CXO 163909.83+565644.1	yes	1639099+565644 ( $J, H, K$ )=15.77(8),15.2(1),14.5(1)	163909.88+565643.6 ( $g, r, i$ )=18.37,17.92,17.47
1RXH J094431.8+573538	no	...	094432.42+573534.9 ( $g, r, i$ )=19.68,20.59,20.11
1RXH J163421.2+570941	yes	163420.44+570944.0 ( $J, H, K$ ) = 8.50(1), 8.04(2), 7.77(2)	... ...

Note. — sat.=saturated. Numbers in parenthesis are the uncertainty in the preceding digits.